European Journal of Medicinal Chemistry
journal homepage: www.elsevier.com

Exploration of Imatinib and Nilotinib-derived Templates as the P2-Ligand for HIV-1 Protease Inhibitors: Design, Synthesis, Protein X-ray Structural Studies, and Biological Evaluation

Arun K. Ghosh [a*], Jennifer L. Mishevich [a], Satish Kovela [a], Ryan Shaktah [a], Ajay K. Ghosh [a], Megan Johnson [a], Yuan-Fang Wang [b], Andres Wong-Sam [b], Johnson Agniswamy [b], Masayuki Amano [e], Yuki Takamatsu [e], Shin-ichiro Hattori [e], Irene T. Weber [b], Hiroaki Mitsuya [c,e,f]

[a] *Department of Chemistry and Department of Medicinal Chemistry, Purdue University, West Lafayette, IN 47907, United States*
[b] *Department of Biology, Georgia State University, Atlanta, Georgia 30303, United States*
[c] *Departments of Infectious Diseases and Hematology, Kumamoto University Graduate School of Biomedical Sciences, Kumamoto 860-8556, Japan*
[d] *Department of Medical Technology, Kumamoto Health Science University, Kumamoto 861-5598, Japan*
[e] *Center for Clinical Sciences, National Center for Global Health and Medicine, Tokyo 162-8655, Japan*
[f] *Experimental Retrovirology Section, HIV and AIDS Malignancy Branch, National Cancer Institute, National Institutes of Health, Bethesda, MD 20892, United States*

ARTICLE INFO

[†] The PDB accession codes for **5b**- and **5c**-bound HIV PR X-ray structures are: 8FUI and 8FUJ, respectively

Keywords:

HIV-1 protease inhibitors, antiviral, imatinib, nilotinib, kinase inhibitors, X-ray crystal structure, backbone binding, pyridylpyrimidine.

ABSTRACT

Structure-based design, synthesis, X-ray structural studies, and biological evaluation of a new series of potent HIV-1 protease inhibitors are described. These inhibitors contain various pyridyl pyrimidine, aryl thiazole or alkylthiazole derivatives as the P2 ligands in combination with darunavir-like hydroxyethylamine sulfonamide isostere. These heterocyclic ligands are inherent to kinase inhibitor drugs, such as nilotinib and imatinib. These ligands are designed to make hydrogen bonding interactions with the backbone atoms in the S2 subsite of HIV-1 protease. Various benzoic acid derivatives have been synthesized and incorporation of these ligands provided potent inhibitors that exhibited subnanomolar level protease inhibitory activity and low nanomolar level antiviral activity. Two high resolution X-ray structures of inhibitor-bound HIV-1 protease were determined. These structures provided important ligand-binding site interactions for further optimization of this class of protease inhibitors.

*Corresponding author:

Department of Chemistry and Department of Medicinal Chemistry
Purdue University, 560 Oval Drive, West Lafayette, IN 47907
Phone: (765)494-5323; Fax: (765)496-1612
E-mail: akghosh@purdue.edu

1. Introduction

Therapeutic inhibition of virally encoded HIV-1 protease is one of the most important strategies for the treatment of HIV-1 infection and AIDS.[1-3] The development of HIV-1 protease inhibitor drugs using protein X-ray structure-based design is regarded as a major achievement in medicinal chemistry.[4,5] Protease inhibitors have been an integral part of current antiretroviral therapies (cART) with reverse transcriptase inhibitors which emerged in the mid-1990s.[6,7] The cART treatment regimens have dramatically transformed HIV/AIDS into a manageable chronic ailment.[8,9,10] As a result, the HIV-related mortality rates continued to decline due to improved treatment regimens.[11,12] Despite these major improvements, the growing emergence of drug-resistant strains, high pill burden and drug side effects are becoming major concerns regarding the long-term prospects of HIV/AIDS management.[13,14,15] In particular, the first generation of HIV-1 protease inhibitors were associated with peptide-like features which contributed to poor oral bioavailability, high metabolic degradation, and other debilitating side effects.[13,16] The development of second generation protease inhibitor drugs alleviated some of these major issues however, current treatments are far from ideal due to the emergence of drug resistance, cardiovascular, and CNS (central nervous system) problems associated with current treatment regimens.[17,18] In our continuing efforts towards the development of improved treatment options, our protease inhibitor design strategy has been aimed at maximizing hydrogen bonding interactions with the active site protease backbone atoms.[19,20] These strategies have resulted in a range of highly potent inhibitors including FDA approved inhibitor drug, darunavir (**1**, Figure 1) and related compound TMC-126 (**2**).[21-24] Darunavir, exhibits a dual mechanism of action in which it inhibits the catalytically active dimeric HIV-1 protease and also inhibits dimerization of the individual protease monomers, preventing the formation of catalytically active protease enzyme.[25,26]

Darunavir utilizes a unique design strategy that involved promoting a network of hydrogen-bonding interactions with protease backbone S2 to S2' sites of the active site.[19,27,28] These properties most likely contributed to darunavir's high genetic barrier to the development of drug-resistant variants compared to other approved protease inhibitor drugs.[29,30] While darunavir is used widely as a first line therapy for rescue treatment, darunavir resistant HIV-1 variants have emerged.[31,32,33] Therefore, further development of a new class of protease inhibitors with structurally novel features are important for future treatment options.

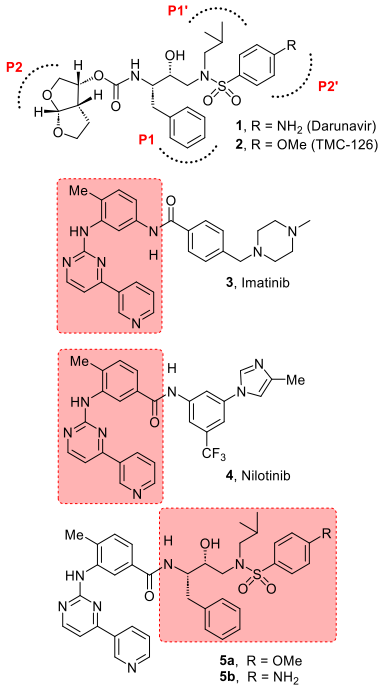

Figure 1. Structure of HIV-1 protease inhibitors **1-5**

One of the important features of darunavir is the bicyclic polyether-like P2 ligand, the *bis*-tetrahydrofuranyl heterocycle.[34,35] Both oxygens of this polyether scaffold form tight hydrogen bonds with backbone amide NHs of Asp29 and Asp30 in the S2 subsite.[27,28] In an effort to design new functionalities that can accommodate similar hydrogen bonding interactions with the backbone atoms, we speculated that the pyridylpyrimidine scaffold of imatinib **3** or nilotinib **4** can be incorporated with substituted 3-aminobenzoic acid to mimic hydrogen bonding interactions in the S2 subsite similar to the *bis*-THF ligand of darunavir.[36,37] Nilotinib is a selective tyrosine kinase receptor inhibitor used for the treatment of chronic myelogenous leukemia. Nilotinib binds to and stabilizes the inactive conformation of the kinase domain of the Abl protein of the Bcr-Abl fusion protein. This results in the inhibition of the Bcr-Abl-mediated proliferation of Philadelphia chromosome-positive (Ph+) chronic myeloid leukemia (CML) cells.[38,39] Nilotinib is orally bioavailable, and incorporation of its structural features may improve pharmacological properties of the resulting protease inhibitors.

The X-ray structural studies of imatinib- and nilotinib-bound Abl-Bcr kinase revealed donor-acceptor abilities of pyridylpirimidine hetereocycles.[40,41] The major advantage is that such heterocyclic ligands would not have stereochemical complexities related to *bis*-THF ligand. We describe here our effort towards the design of a new class of HIV-1 protease inhibitors by incorporating a variety of hinge-binding heterocycles that would maintain the critical hydrogen bonding interactions in the S2 subsite of HIV-1 protease. The structural class is represented in compound **5**. These heterocyclic scaffolds are key templates for kinase inhibitor drugs, imatinib and dasatinib. For our preliminary work, we investigated the new ligand scaffolds in combination with the hydroxyethylamine sulfonamide isostere inherent to darunavir and TMC-126.[19, 22]

2. Results and discussion

We recently reported a series of HIV-1 protease inhibitors that incorporated substituted isophthalamide derivatives as the P2-ligands.[42,43] A representative example inhibitor **6** is shown in Figure 2. These inhibitors were designed by taking advantage of the large hydrophobic pocket in the HIV-1 protease S1-S2 subsites.[43] While the P2-ligands resemble 3-hydroxy-2-methyl benzamide inherent to nelfinavir **7**, an FDA approved drug, X-ray structural studies of inhibitor-bound HIV-1 protease revealed that the 3-hydroxy benzylamide carbonyl involved in hydrogen bonding interaction with the backbone amide NH of Asp29.[44,45] However, the oxazolylmethyl segment is mostly solvent exposed and does not participate in any polar interactions in the actve site. Based upon this structural precedence, we planned to investigate pyridyl pyrimidine and various alkyl,

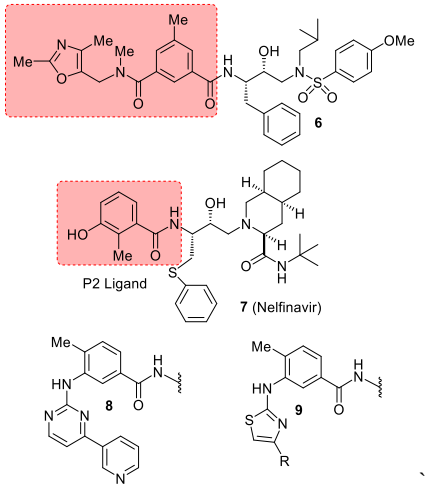

Figure 2. Structure of HIV-1 protease inhibitors and ligands

arylthiazolyl hetereocycles such as **8** and **9** in combination with hydroxyethylamine sulfonamide isosteres. Our preliminary models of pyridyl pyrimidine derivatives, based upon the X-ray structure of nelfinavir-bound HIV-1 protease, revealed that pyridyl pyrimidine functionalities can form hydrogen bonds with backbone amide NHs in the S2 subsite.[45] Also, we speculated that appropriately functionalized alkyl or aryl substituents can effectively fill in the hydrophobic pocket in the S2-S3 subsites. There is no previous report of the use of pyridyl pyrimidine derived P2 ligands in the design of HIV-1 protease inhibitors.

2.1 Synthesis of inhibitors

The synthesis of various nilotinib-based HIV-1 protease inhibitors **5a-d** is shown in Scheme 1. Commercially available 4-methyl-3-[[4-(3-pyridinyl)-2-pyrimidinyl]amino]benzoic acid **10** was reacted with previously reported hydroxyethylene isosteres **11-14** in the presence of HATU and Et_3N in DMF at 23 °C for 24 h to afford the desired coupling products **5a-d** in good yield (60-76%). The syntheses of various methyl-3-[[4-(3-pyridinyl)-2-thiazolyl]amino]benzoic acids and syntheses of

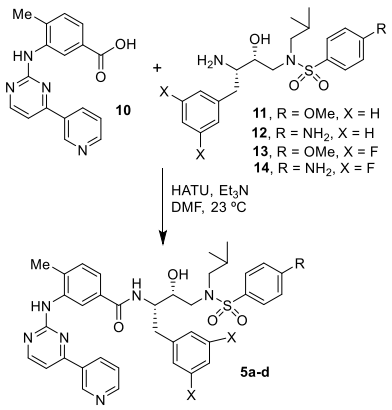

Scheme 1. Synthesis of protease inhibitors **5a-d**.

inhibitors **5e-i** are shown in Scheme 2. Hantzsch thiazole synthesis[46] was utilized in order to obtain these desired pyridinyl-thiazolylamino benzoic acid derivatives. As shown, varius methylsubstituted aminomethylbenzoates **15** were reacted with potassium thiocyante and acetyl chloride in acetone at 23 ºC to 60 ºC to provide thiourea derivatives **16**. Exposure of **16** to potassium carbonate in methanol, followed by addition of α-bromo ketone **17** furnished pyridinylthiazole derivatives **18**. Saponification of methyl esters **18** with 1 M LiOH in THF at 23 ºC afforded ligand carboxylic acids **19a-e**. Coupling of these ligand acids with hydroxyethylsulfonamide isosteric amine **11**[22, 34] provided inhibitors **5e-i** in good yields.

The synthesis of various methyl substituted thiazole ligands and their conversion to inhibitors **5j-m** are shown in Scheme 3. Methyl thiazole derivatives **20a-d** were synthesized utilizing an efficient one step procedure reported by Lagoja and Schantl.[47] This procedure involves reaction of potassium thiocyanate with chloroacetone at 23 ºC followed by addition of amino methyl esters **15a-d** and heating to 60 ºC in methanol for 6 h to provide **20a-d**. The procedure resulted in good yields of these thiazole derivatives. However, yields are lower if the reactions are carried out longer than 6 h. Saponification of methyl esters **20** with 1 M LiOH in THF at 23 ºC provided carboxylic acids **21a-d**. Coupling of these ligand acids with amine **11** as described above provided inhibitors **5j-m** in good yields.

The synthesis of trifluoromethyl and methoxymethyl substituted thiazole ligand acids and their conversion to inhibitors **5n-p** are shown in Scheme 4. For the synthesis of trifluoromethyl substuted ligand acids, thiourea derivatives **16a** and **16b** were reacted with trifluoromethyl ketone **22** to provide thiazole ester derivatives **23a** and **23b**. Saponification of the methyl esters furnished ligand acids **24a** and **24b**. Coupling of these acids with amine **11** resulted inhibitors **5m** and **5n,** respectively. Methoxymethyl

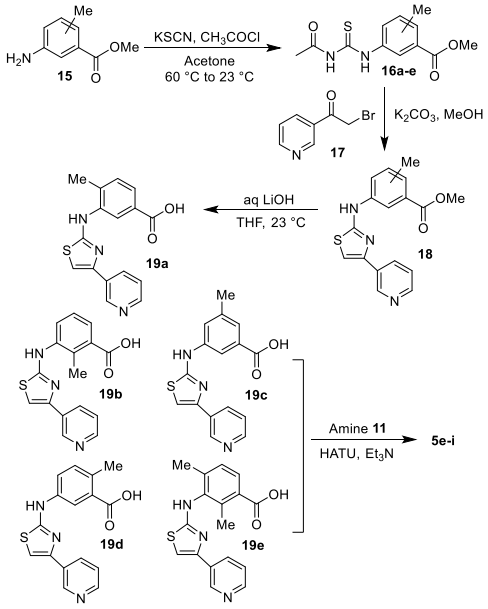

Scheme 2. Synthesis of protease inhibitors **5e-i**.

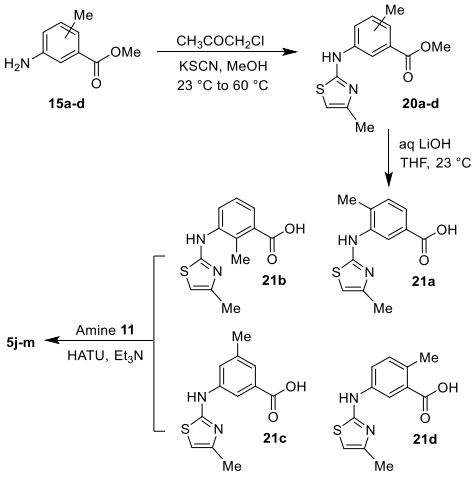

Scheme 3. Synthesis of protease inhibitors **5j-m**.

substituted thiazole ligand acid was synthesized from thiourea derivative **16d** and the known α-bromo ketone **25**, which was prepared using the reported procedure.[48] This bromo ketone derivative is known to undergo Favorskii rearrangement upon heating, standing, or in the presence of base to provide the undesired secondary α-bromide.[48] We therefore employed freshly prepared bromo ketone. The reaction of **25** with thiourea **16d** was carried out with lower equivalents of potassium carbonate. The thiazole derivative **26** was obtained in low yield possibly due the extreme base sensitivity. Saponification of ester **26** followed by coupling of the resulting acid **27** with amine **11** afforded inhibitor **5p**.

2.2 Biological evaluation and structure-activity relationship

We first investigated the ability of the nilotinib subunit, pyridinyl-pyrimidinyl amino benzamides to serve as P2 ligands in the S2 subsite of HIV-1 protease. The structure and activity of these inhibitors are shown in Table 1. The HIV-1 protease inhibitory activity of these compounds was evaluated in an enzyme-inhibitory assay reported by Toth and Marshall.[49]

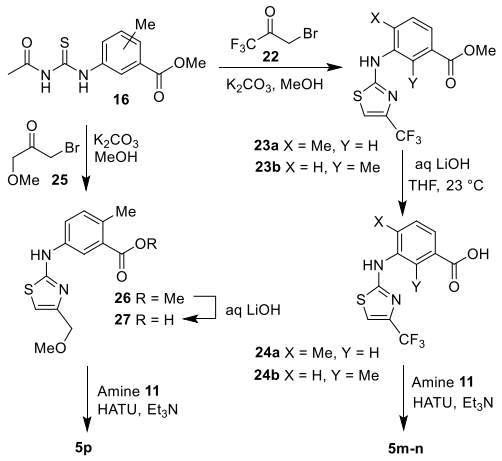

Scheme 4. Synthesis of protease inhibitors **5m-p**.

As shown, compound **5a** with a nilotinib pyridinyl-pyrimidinyl heterocycle as the P2 ligand and 4-methoxy sulfonamide as P2'-ligand exhibited very potent HIV-1 protease inhibitory activity with a K_i of 0.028 nM. The corresponding 4-aminosulfonamide derivative **5b** displayed nearly 5-fold reduction in inhibitory K_i value (entry 2). We also determined the antiviral activity of these inhibitors in MT-2 human-T-lymphoid cells exposed to HIV_{LAI}.[50] In this antiviral assay, compound **5a** showed a potent antiviral IC_{50} value of 154 nM. Interestingly, compound **5b** showed a further improvement in antiviral activity compared to its 4-methoxy derivative, **5a**. Compound **5c** with 3,5-difluorophenylmethyl as the P1 ligand did not improve inhibitory activity and showed only a slight improvement in antiviral activity over compound **5a** (entry 3). The corresponding 4-amino derivative **5d** did not improve activity over compound **5b**. Interestingly, compound **5d** exhibited 3-fold reduction in antiviral activity over compound **5c** (entries 3 and 4). We then examined a pyridyl thiazole heterocycle in place of the pyridyl pyrimidinyl scaffold in compounds **5a-d**. Compound **5e**, with a 4-methylbenzamide scaffold showed reduced inhibitory activity compared to its pyridylpyrimidine derivative **5a**. This compound showed antiviral IC_{50} value of 390 nM. The 2-methyl-3-aminothiozolyl derivative **5f** displayed an enzyme inhibitory K_i of 19 nM but did not exhibit any appreciable antiviral activity (entry 6). Compound **5g** with a 3-aminothiazoloyl-5-methyl heterocycle did not improve any activity (entry 7). Such discrepancies between activity in enzyme and antiviral assays are common possibly due to poor cell membrane permeability of compounds **5f** and **5g**. Interestingly, 3-aminothiazoloyl-6-methyl derivative **5h** showed an improvement in K_i value (8.7 nM). Also, this compound showed an antiviral IC_{50} value of 580 nM (entry 8). Compound **5i** with a 2,4-dimethyl-3-aminothiazolyl derivative showed reduction in K_i value, but maintained an antiviral IC_{50} of 510 nM, comparable to derivative **5h** (entries 8, 9).

We then investigated the effect of alkyl substitution on the 3-thiazolyl group as well as methyl substitution on the benzamide scaffold. The structure and activity of various derivatives are shown in Table 2. Compound **5j** with a 3-methyl-thiazolylamino heterocycle showed a slight improvement in HIV-1 inhibitory activity (K_i value 26 nM) over the corresponding 3-pyridine derivative **5e**. However, it did not show any appreciable antiviral activity (entry 1). We have examined the effect of methyl substitution on the benzamide ring. Compounds **5k-m** with 2-methyl, 5-methyl, and 6-methyl substitutions resulted in no improvement of activity over 4-methyl derivative **5j** (entries 1-4). Also, substitution of a 2-trifluoromethyl group in compounds **5n** and **5o** did not improve any activity over their methyl derivatives (entries 5 and 6). Incorporation of a methoxy group on the 2-methyl derivative in compound **5p** showed a slight improvement in inhibitory activity. This compound also exhibited antiviral activity IC_{50} value of 630 nM (entry 7). Our X-ray crystallographic studies of inhibitor **5b**-bound HIV-1 protease provided molecular insight into the ligand-binding site interactions responsible for its inhibitory properties.

Table 1. Structure and activity of pyrimidine- and thiozole-derived protease inhibitors

Entry	Inhibitor	K_i (nM)[a]	IC_{50} (nM)[b]
1.	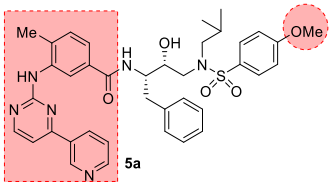 5a	0.028	154
2.	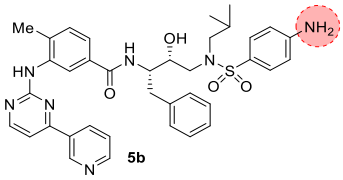 5b	0.17	66.8
3.	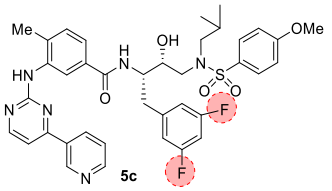 5c	0.58	124
4.	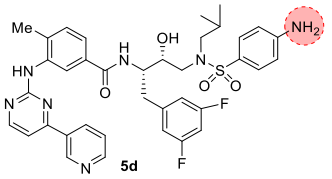 5d	1.92	212
5.	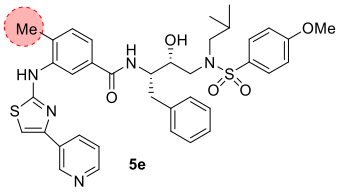 5e	38.3	390
6.	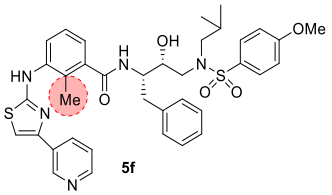 5f	19.3	>1

7.	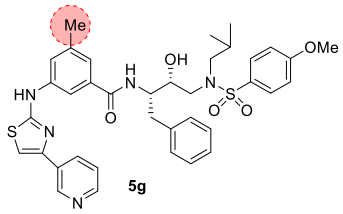 5g	185.2	>1
8.	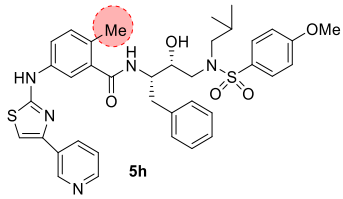 5h	8.7	580
9.	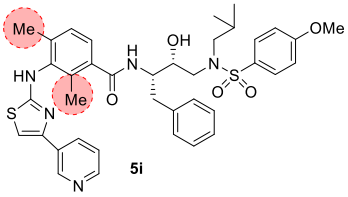 5i	122	510

[a]Ki values represents at least 5 data points. Standard error in all cases was less than 7%. Darunavir exhibited K_i = 16 pM. [b]Values are means of at least three experiments. Standard error in all cases was less than 5%. Darunavir exhibited IC_{50} = 2.1 nM.

Table 2. Structure and activity of substituted thiazolyl-derived protease inhibitors

Entry	Inhibitor	K_i (nM)[a]	IC_{50} (nM)[b]
1.	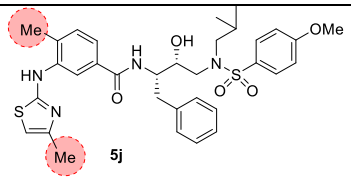 5j	26.5	>1
2.	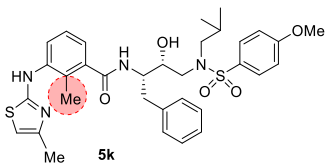 5k	71.9	>1
3.	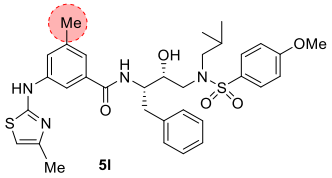 5l	80.0	>1
4.	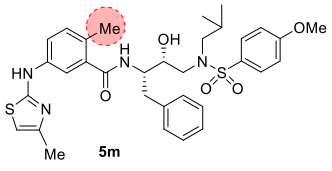 5m	75.9	>1
5.	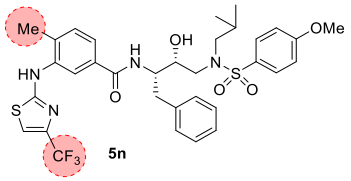 5n	60.3	>1
6.	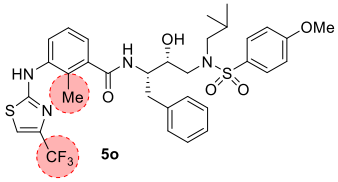 5o	72	>1
7.	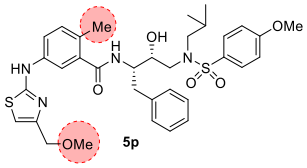 5p	18.0	630

[a]Ki values represents at least 5 data points. Standard error in all cases was less than 7%. Darunavir exhibited K_i = 16 pM. [b]Values are means of at least three experiments. Standard error in all cases was less than 5%. Darunavir exhibited IC_{50} = 2.1 nM.

2.3 X-ray structural studies

The X-ray structures of inhibitors **5b** and **5c** were determined in complex with wild-type HIV-1 protease at 1.25 Å and 1.12 Å, respectively.[51] Both complexes crystallized in the orthorhombic space group $P2_12_12$ with one protease homodimer per asymmetric unit. The inhibitors were observed in the active site in two alternate conformations related by 180° rotation with relative occupancy of 0.65/0.35 and 0.55/0.45, respectively. These conformations are depicted in Figure 2 and the 2Fo-Fc electron density maps showing the alternative conformations are in the Supplemental Material. Crystal structures of HIV protease with inhibitors frequently have alternate conformations for inhibitor bound in two orientations due to the pseudo-symmetrical arrangement of the two subunits in the protease dimer. In most cases, the two conformations are almost identical and show very similar interactions with the protease. However, unlike most of the reported X-ray structures of HIV protease, the two conformations of inhibitors **5b** and **5c** formed different interactions with HIV protease and nearby solvent molecules. In particular, inhibitor **5b** had an unusually large difference in the two conformations for the P2-P3 rings. Conformation A has higher relative occupancy of 0.65 which suggests the A conformation is preferred over the B conformation. The protease dimers in **5b**- and **5c**-HIV protease complexes share similar backbone structures with HIV-1 PR/darunavir (DRV) complex [27,28] with a low RMSD of 0.13 Å and 0.17 Å, respectively, for superposition of 198 equivalent Ca atoms. The largest deviation of 0.5 Å occurred at residue Gly49' in **5b**-bound HIV-1 protease structure, and 0.7 Å at Ala71' in **5c**-bound HIV-1 protease structure. Both inhibitors formed similar hydrogen bond interactions to those observed between DRV and the main chain atoms of HIV-1 protease. The key interactions of inhibitor **5b** with HIV-1 protease and inhibitor **5c** with HIV-1 protease are highlighted in stereoviews of the active sites in Figures 3 and 4, respectively. As in many HIV protease structures, both inhibitors also formed a tetracoordinated water-mediated hydrogen bond interaction with one of the sulfonamide oxygens, the carbonyl oxygen and the amide nitrogen of flap residues Ile50 and Ile50´.[4,5]

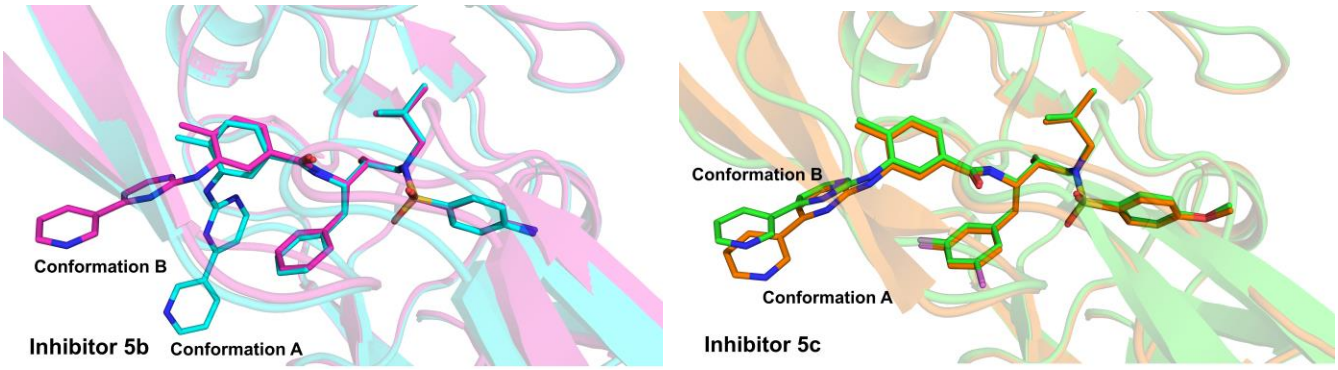

Figure 2. Superimposed conformations of inhibitors **5b** and **5c** in the HIV-1 protease active site. **5b**: conformation A in turquoise and conformation B in magenta with relative occupancies of 0.65 and 0.35 (PDB code, **5b** : 8FUI); **5c**: conformation A in orange and conformation B in green with relative occupancies of 0.55 and 0.45 (PDB code, **5c** : 8FUJ).

Both inhibitors **5b** and **5c** are quite different from darunavir as the *bis*-THF, P2 ligand is replaced with a P2-P3 group which contains three linked aromatic rings, a 4-methyl-benzamide, a pyrimidine, and a pyridine moeity. The 4-methyl-benzamide group is closest to the P1 group of the inhibitor, the pyrimidine group is in the center, and the pyridine group is the outermost ring. Other modifications were introduced in inhibitor **5c** which contains a methoxyl group in place of the aniline NH_2 in the P2' ligand of DRV, and a 3,5-difluorophenylmethyl moiety replaces the P1 phenyl ligand in DRV. These altered P1 and P2' groups show similar interactions with protease as described for the corresponding groups in other inhibitors.[52,53] For both inhibitors, the outer two rings occur in two distinct conformations for the two orientations of the inhibitor due to different rotations of the flexible connections combined with weaker interactions formed with the protease. In conformation A of inhibitor **5b**-bound HIV-1 protease structure, the outer two rings (P3) are rotated toward Asp29 and Arg8' and stabilized by π-π stacking interactions. In conformation B, the outer rings are rotated toward the flap region and form weak C-H...O with Gly48 and the carbonyl oxygen of Met46. The 4-methyl-benzamide is a mimic of 4-aminobenzene at P2', however, the methyl group of 4-methyl-benzamide in P2-P3 does not coincide with the position of the amide (N1) of the P2' ligand on 180° rotation, but is shifted by 1.6 Å and 1.2 Å, respectively, in the two orientations of inhibitor.

The hydrogen bond interactions of inhibitor **5b** with HIV protease are shown in Figure 3. The interactions between the P2-P3 group in inhibitor **5b** and protease include standard hydrogen bonds and multiple weaker interactions, such as C-H...O and π-π stacking interactions. The geometrical criteria used to define the weaker interactions are stated in the Supporting information. As shown in Figure 3, the N62 atom of the pyrimidine group forms a hydrogen bond with the amine of Asp29 at 3.2 Å. The 4-methyl-benzamide group forms additional C-H…π interactions with Ala28. A chlorine ion in the solvent interacts with atom N60 of the 4-methyl benzamide group and the amine of Gly48 at distances of 3.3 Å and 3.2 Å, respectively. The pyrimidine N66 of the pyrimidine group forms a hydrogen bond with a water molecule, while C76 forms a C-H…O interaction with a second water. The first water forms a direct hydrogen bond with the carbonyl oxygen atom of Gly48, and the second water interacts via a network of other waters with the side chains of Glu21' and Arg8'. The pyrimidine and pyridine rings form additional π-π stacking interactions with the carboxylic oxygen of Asp29 and the guanidine of Arg8'. The pyrimidine of P2-P3 also forms internal π-π stacking interactions with the P1 phenyl of the inhibitor. Additional C-H…π interactions also occur with Val82'. These favorable interactions were omitted from Figure 3 for clarity.

In conformation B of inhibitor **5b** and in both orientations of inhibitor **5c** in Figure 4, the N60 atom of the 4-methyl-benzamide group forms a hydrogen bond with the carbonyl oxygen of Gly48 at 2.8-3.0 Å. A water molecule mediates hydrogen bond interactions between the N62 atom of the pyrimidine group and the amine atom of Asp29. The 4-methyl-benzamide group is sandwiched between the carbonyl oxygen atoms of Asp30 and Gly48 via C-H...O interactions at distances of 3.5 Å and 3.2 Å, respectively in conformation B of inhibitor **5b**. In both orientations of inhibitor **5c**, similar interactions with Gly48 are maintained at distances of 3.0-3.1 Å. The pyrimidine group of the N66 atoms forms a hydrogen bond with the amine of Gly48 at 3.0-3.3 Å distance, while the C63 atom of the pyrimidine group forms a C-H...O interaction with the side chain carboxylate of Asp29.

Several other weak interactions link the P2-P3 group of inhibitor with the protease. C-H...π interactions connect the 4-methyl-benzamide group

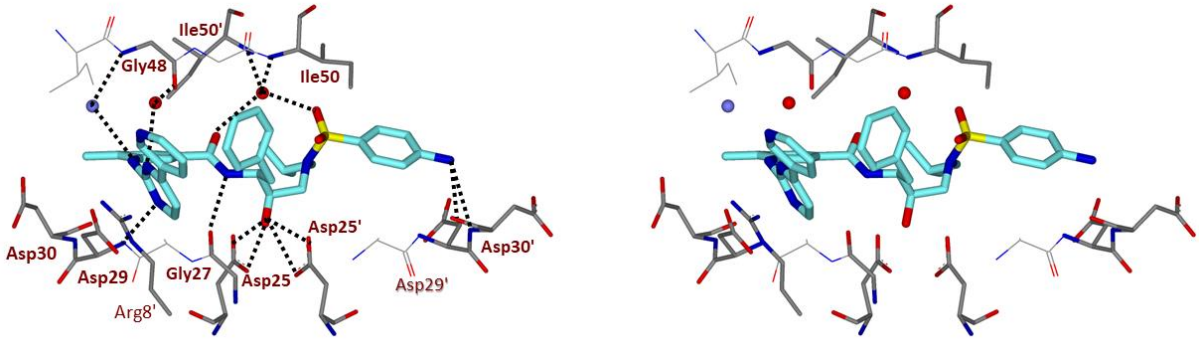

Figure 3. Stereoview of the X-ray crystal structure of inhibitor **5b** (turquoise) conformation A into the active site of HIV-1 protease (PDB code: 8FUI). The pyridylpyrimidine P2 ligand makes several hydrogen bonds in the S2 subsite. Hydrogen bond interactions were defined by standard geometric criteria. All key hydrogen bonds are shown as black dotted lines.

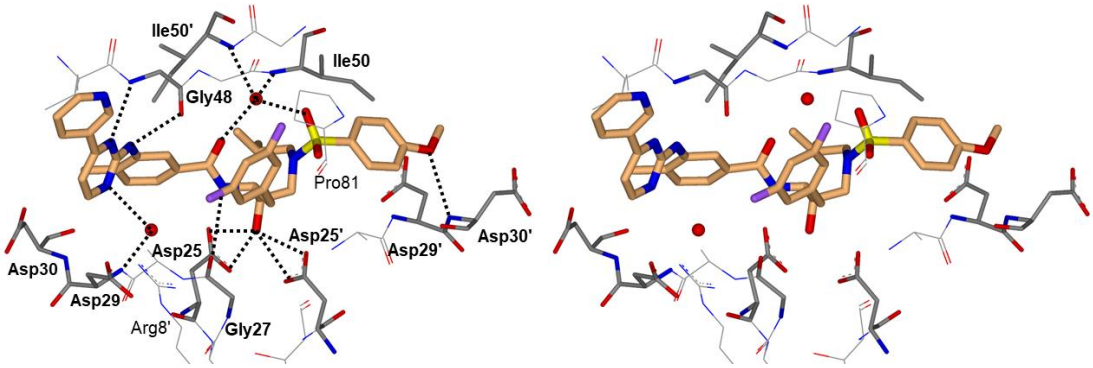

Figure 4. Stereoview of the X-ray crystal structure of inhibitor **5c** (orange) conformation A into the active site of HIV-1 protease (PDB code: 8FUJ). The pyridylpyrimidine P2 ligand makes interesting hydrogen bonds in the S2 subsite. Hydrogen bond interactions were defined by standard geometric criteria. All key hydrogen bonds are shown as black dotted lines

with Ala28 sidechain and the pyrimidine group with the Ile47 sidechain. Two water molecules form O-H..π interactions with the pyrimidine group and the pyridine group, however, the second water interaction with the pyridine group is lost in one conformation of inhibitor **5c**. The carbonyl oxygen atom of Met46 forms a lone-pair...π interaction with the pyridine group at 3.2-3.8 Å. One parallel-displaced π-π stacking interaction is formed between the pyrimidine group and the carboxylic group of Asp30. Therefore, both inhibitors can attain multiple interactions with protease due to the distinct conformations of the P2-P3 rings. These interactions are responsible for the high affinity of inhibitors **5b** and **5c** by the HIV-1 protease.

3. Conclusion

In summary, we have designed and synthesized a new class of HIV-1 protease inhibitors incorporating the pyridyl pymiridine nilotinib subunit and aryl thiazole derivatives of dasatinib as the P2 ligands. We have examined the activity profiles of methyl thiazole derivatives. Also, we examined the effect of methyl substitution on the benzamide ring. Various alkyl and aryl thiazoles were conveniently prepared using Hantzsch thiazole synthesis. Several compounds exhibited very potent enzyme inhibitory activity in low nanomolar to subnanomolar level. A number of compounds also displayed low nanomolar antiviral activity. In general, pyridyl pymiridine benzamide derivatives provided the most promising results. Compound **5a** with a 4-methoxysulfonamide as the P2'-ligand turned out be the most potent compound, which exhibited an enzyme inhibitory K_i of 28 pM and antiviral activity of 154 nM. Compound **5b** with a 4-aminosulfonamide as the P2'-ligand displayed potent antiviral activity with IC_{50} value of 66 nM. Incorporation of lipophilic 1,3-difluorophenyl P1-ligand did not improve antiviral activity. Among thiazole derived inhibitors, compound **5h** with a pyridyl thiazole as the P2 ligand showed the best result exhibiting an HIV-1 protease inhibitory K_i of 8.7 nM and antiviral activity of 580 nM. Methyl thiazole-derived compounds showed low nanomolar HIV-1 protease activity but no appreciable antiviral activity. Inhibitors **5a** and **5b** differ only in the presence of OMe instead of NH2 in the P2' ligand, although the conformations of the P2-P3 rings may differ to an unknown extent and influence the binding potency. Our X-ray structural studies of inhibitor **5b**-bound HIV-1 protease provided intriguing molecular insight into their ligand-binding site interactions. As it turns out, one of the pyrimidine nitrogens forms a hydrogen bond with the backbone amide NH of Asp29. The pyrimidine group also forms additional C-H...π interactions with Ala28. Also, the other pyrimidine nitrogen forms a water mediated hydrogen bond with the amide NH of Gly48, located in the flap region of HIV-1 protease. Moreover, the pyrimidine and pyridine rings make favorable π-π and C-H...π interactions with protease side chains. In contrast, inhibitor **5c** cannot form these interactions likely due to steric hindrance from the fluorines on P1 phenyl, which may explain its lower potency. The preliminary results of these pyridyl pyrimidine-derived inhibitors are very encouraging and warrant further optimization of ligand-binding site interactions. We are utilizing these current results for further improvement of inhibitor properties.

4. Experimental Section

All moisture-sensitive reactions were carried out in oven-dried glassware under an argon atmosphere unless otherwise stated. Anhydrous solvents were obtained as follows: Tetrahydrofuran was distilled from sodium metal/benzophenone under argon. Dichloromethane was distilled from calcium hydride under argon. All other solvents were reagent grade. Column chromatography was performed using Silicycle Silia Flash F60 230 – 400 mesh silica gel. Thin layer chromatography was carried out using EMD Millipore TLC silica gel 60 F254 plates. ^{1}H NMR and ^{13}C NMR spectra were recorded on a Bruker AV-III-400, Bruker DRX500, or Bruker AV-111-800. Low-resolution mass spectra were collected on an LCMS. High-resolution mass spectra were collected by the Purdue University Campus-Wide Mass Spectrometry Center. HPLC analysis and purification were done on an Agilent 1100 series instrument using a YMC-Pak ODS-A column of 4.6 mm i.d. for analysis and either 10 mm i.d. or 20 mm i.d. for purification. The purity of all test compounds was determined by HPLC analysis to be >90% pure.

N-((2S,3R)-3-hydroxy-4-((N-isobutyl-4-methoxyphenyl)sulfonamido)-1-phenylbutan-2-yl)-4-methyl-3-((4-(pyridin-3-yl)pyrimidin-2-yl)amino)benzamide **(5a).** To a stirring solution of commercially available carboxylic acid **10** (15 mg, 0.05 mmol) in DMF (1 mL) was added triethylamine (0.05 mL, 0.35 mmol), HATU (29 mg, 0.08 mmol), and amine **11** (0.06 mmol). The reaction was then stirred for 24 h at 23 °C. The reaction mixture was concentrated under reduced pressure and purified via silica gel column chromatography (70% EtOAc/hexanes) to afford **5a** (22 mg, 76%): ^{1}H NMR (500 MHz, $CDCl_3$) δ 9.30 (s, 1H), 8.73 (d, J = 4.7 Hz, 1H), 8.62 (s, 1H), 8.51 (dd, J = 5.2, 0.8 Hz, 1H), 8.35 (dt, J = 7.9, 2.0 Hz, 1H), 7.72 – 7.66 (m, 2H), 7.45 (dd, J = 8.0, 4.8 Hz, 1H), 7.32 – 7.10 (m, 7H), 6.95 – 6.89 (m, 2H), 6.54 (d, J = 8.4 Hz, 1H), 4.42 (dt, J = 7.4, 3.7 Hz, 1H), 4.08 (dt, J = 8.0, 4.0 Hz, 1H), 3.82 (s, 3H), 3.22 (dd, J = 15.0, 4.2 Hz, 1H), 3.14 – 3.00 (m, 3H), 2.94 (dd, J = 13.5, 7.7 Hz, 1H), 2.84 (dd, J = 13.4, 7.3 Hz, 1H), 2.38 (s, 3H), 1.90 (dq, J = 13.7, 6.8 Hz, 1H), 0.85 (dd, J = 11.7, 6.6 Hz, 6H);^{13}C NMR (125 MHz, $CDCl_3$) δ 168.10, 163.01, 162.64, 160.45, 159.31, 151.56, 148.44, 138.23, 137.76, 134.87, 133.12, 131.45, 130.88, 130.42, 129.61, 129.59, 128.67, 126.63, 124.05, 121.93, 119.21, 114.38, 108.69, 72.65, 58.68, 55.69, 54.55, 53.69, 35.02, 29.84, 27.25, 20.23, 20.19, 18.30; LRMS-ESI (*m/z*): [M+H] 695.3. HRMS (ESI) *m/z*: [M+H] calcd $C_{38}H_{42}N_6O_5SH$ 695.30157; found 695.30138.

N-((2S,3R)-4-((4-amino-N-isobutylphenyl)sulfonamido)-3-hydroxy-1-phenylbutan-2-yl)-4-methyl-3-((4-(pyridin-3-yl)pyrimidin-2-yl)amino)benzamide **(5b).** Inhibitor **5b** was synthesized according to the

same procedure as inhibitor **5a** utilizing carboxylic acid **10** (12 mg, 0.04 mmol), DMF (1 mL), DIPEA (0.04 mL, 0.24 mmol), HATU (20 mg, 0.05 mmol), and amine **12** (0.05 mmol). The crude product was purified via silica gel column chromatography (5% methanolic ammonia/CH_2Cl_2) to afford **5b** (20 mg, 74%): ^{1}H NMR (500 MHz, $CDCl_3$) δ 9.31 (s, 1H), 8.74 (d, *J* = 4.8 Hz, 1H), 8.62 (s, 1H), 8.53 (d, *J* = 5.1 Hz, 1H), 8.37 (dt, *J* = 8.1, 2.0 Hz, 1H), 7.54 (d, *J* = 8.4 Hz, 2H), 7.46 (dd, *J* = 8.0, 4.8 Hz, 1H), 7.36 – 7.16 (m, 8H), 7.13 (s, 1H), 6.63 (d, *J* = 8.4 Hz, 2H), 5.16 (d, *J* = 9.0 Hz, 1H), 4.45 (td, *J* = 7.3, 3.8 Hz, 1H), 4.18 (s, 2H), 4.10 (dt, *J* = 8.2, 4.2 Hz, 1H), 3.30 – 3.04 (m, 4H), 2.88 (ddd, *J* = 50.0, 13.4, 7.5 Hz, 2H), 2.40 (s, 3H), 1.95 – 1.89 (m, 1H), 0.88 (dd, *J* = 10.3, 6.5 Hz, 6H); ^{13}C NMR (125 MHz, $CDCl_3$) δ 168.07, 162.64, 160.49, 159.36, 151.64, 150.74, 148.51, 138.28, 137.75, 134.77, 133.12, 132.62, 131.59, 130.84, 129.61, 129.58, 128.62, 126.64, 126.57, 123.99, 121.91, 119.39, 114.17, 108.68, 72.74, 58.83, 54.49, 54.41, 53.79, 35.03, 27.28, 20.24, 18.28, 14.24; LRMS-ESI (*m/z*): [M+H] 680.3. HRMS (ESI) *m/z*: [M+H] calcd $C_{37}H_{41}N_7O_4SH$ 680.30189; found 680.30245.

N-((2S,3R)-1-(3,5-difluorophenyl)-3-hydroxy-4-((N-isobutyl-4-methoxyphenyl)sulfonamido)butan-2-yl)-4-methyl-3-((4-(pyridin-3-yl)pyrimidin-2-yl)amino)benzamide **(5c).** Inhibitor **5c** was synthesized according to the same procedure as inhibitor **5a** utilizing carboxylic acid **10** (15 mg, 0.05 mmol), DMF (1 mL), DIPEA (0.05 mL, 0.29 mmol), HATU (25 mg, 0.06 mmol), and amine **13** (0.06 mmol). The crude product was purified via silica gel column chromatography (30% acetone/hexanes) to afford **5c** (15 mg, 41%): ^{1}H NMR (500 MHz, $CDCl_3$) δ 9.34 (d, *J* = 2.3 Hz, 1H), 8.77 – 8.68 (m, 2H), 8.53 (d, *J* = 5.1 Hz, 1H), 8.33 (dt, *J* = 8.1, 1.9 Hz, 1H), 7.75 – 7.67 (m, 2H), 7.46 (dd, *J* = 8.0, 4.8 Hz, 1H), 7.29 (dd, *J* = 8.9, 7.1 Hz, 1H), 7.21 (dd, *J* = 5.2, 1.9 Hz, 1H), 7.10 (s, 1H), 6.97 – 6.92 (m, 2H), 6.90 – 6.81 (m, 2H), 6.66 – 6.56 (m, 1H), 5.52 (s, 1H), 4.41 (dt, *J* = 8.9, 4.7 Hz, 1H), 4.10 (s, 1H), 3.83 (s, 3H), 3.23 – 3.16 (m, 1H), 3.14 – 2.94 (m, 4H), 2.84 (dd, *J* = 13.4, 7.1 Hz, 1H), 2.40 (s, 3H), 1.89 (dt, *J* = 13.9, 6.9 Hz, 1H), 0.87 (dd, *J* = 18.6, 6.5 Hz, 6H); ^{13}C NMR (125 MHz, $CDCl_3$) δ 168.10, 164.12, 164.01, 163.11, 162.56, 160.40, 159.44, 151.64, 148.50, 142.63, 137.88, 134.77, 132.67, 131.02, 130.25, 129.59, 124.03, 121.89, 118.33, 114.44, 112.55, 112.36, 108.80, 102.14, 72.57, 58.86, 55.72, 53.99, 53.74, 34.72, 27.29, 20.22, 18.30; LRMS-ESI (*m/z*): [M+H] 731.2. HRMS (ESI) *m/z*: [M+H] calcd $C_{38}H_{40}F_2N_6O_5SH$ 731.28272; found 731.28315.

N-((2S,3R)-4-((4-amino-N-isobutylphenyl)sulfonamido)-1-(3,5-difluorophenyl)-3-hydroxybutan-2-yl)-4-methyl-3-((4-(pyridin-3-yl)pyrimidin-2-yl)amino)benzamide **(5d).** Inhibitor **5d** was synthesized according to the same procedure as inhibitor **5a** utilizing carboxylic acid **10** (15 mg, 0.05 mmol), DMF (1 mL), triethylamine (0.05 mL, 0.29 mmol), HATU (24 mg, 0.06 mmol), and amine **14** (0.06 mmol). The crude product was purified via silica gel column chromatography (50% acetone/hexanes) to afford **5d** (32 mg, 89%): ^{1}H NMR (500 MHz, $CDCl_3$) δ 9.32 (d, *J* = 2.3 Hz, 1H), 8.74 (dd, *J* = 4.8, 1.6 Hz, 1H), 8.67 (d, *J* = 2.0 Hz, 1H), 8.52 (d, *J* = 5.1 Hz, 1H), 8.33 (dt, *J* = 8.1, 1.9 Hz, 1H), 7.57 – 7.51 (m, 2H), 7.45 (dd, *J* = 8.0, 4.8 Hz, 1H), 7.29 (dd, *J* = 10.4, 8.5 Hz, 1H), 7.21 (dd, *J* = 5.2, 1.9 Hz, 1H), 7.10 (s, 1H), 6.87 – 6.83 (m, 2H), 6.66 – 6.57 (m, 3H), 5.37 (s, 1H), 4.41 (dd, *J* = 7.3, 3.6 Hz, 1H), 4.13 (s, 2H), 4.08 (s, 1H), 3.18 (dd, *J* = 15.0, 4.5 Hz, 1H), 3.14 – 2.88 (m, 4H), 2.80 (dd, *J* = 13.4, 7.1 Hz, 1H), 2.39 (s, 3H), 1.94 – 1.82 (m, 1H), 0.87 (dd, *J* = 16.1, 6.6 Hz, 6H); ^{13}C NMR (125 MHz, $CDCl_3$) δ 168.07, 162.61, 160.44, 159.41, 151.67, 150.76, 148.50, 142.60, 137.87, 134.77, 133.01, 132.66, 131.26, 131.00, 129.61, 126.61, 124.02, 121.90, 118.67, 114.23, 112.55, 112.36, 108.78, 102.10, 72.70, 59.02, 54.01, 53.82, 34.76, 29.84, 27.34, 20.24, 18.31; LRMS-ESI (*m/z*): [M+H] 716.3. HRMS (ESI) *m/z*: [M+H] calcd $C_{37}H_{39}F_2N_7O_4SH$ 716.28306; found 716.28351.

N-((2S,3R)-3-hydroxy-4-((N-isobutyl-4-methoxyphenyl)sulfonamido)-1-phenylbutan-2-yl)-4-methyl-3-((4-(pyridin-3-yl)thiazol-2-yl)amino)benzamide **(5e).** To a stirring solution of **19a** (16.5 mg, 0.05 mmol) in CH_2Cl_2 (1.0 mL) was added triethylamine (0.04 mL, 0.32 mmol) and HATU (26.0 mg, 0.07 mmol) at 23 °C. To the reaction was then added **11** (0.058 mmol) and the reaction was stirred for 24h. The reaction mixture was washed with 1 M citric acid and then successively with H_2O. The organic layer was then washed with brine, dried over Na_2SO_4, filtered and concentrated under reduced pressure. The crude product was purified via silica gel column chromatography (40-45% EtOAc/hexanes) to afford **5e** (11 mg, 29.7%): ^{1}H NMR (500 MHz, $CDCl_3$) δ 9.12 (d, *J* = 1.8 Hz, 1H), 8.51 (d, *J* = 5.9 Hz, 1H), 8.24 (s, 1H), 8.06 (d, *J* = 8.0 Hz, 1H), 7.68 (d, *J* = 8.8 Hz, 2H), 7.46 (bs, 1H), 7.33 - 7.23 (m, 6H), 7.16 (t, *J* = 7.3 Hz, 1H), 6.95 – 6.87 (m, 3H), 6.72 (d, *J* = 8.4 Hz, 1H), 4.46 - 4.38 (m, 1H), 4.1 – 4.06 (m, 1H), 3.83 (s, 3H), 3.22 – 3.04 (m, 4H), 2.95 – 2.78 (m, 2H), 2.34 (s, 3H), 1.93 – 1.81 (m, 1H), 0.85 (t, *J* = 6.4 Hz, 6H); ^{13}C NMR (125 MHz, $CDCl_3$) δ 167.66, 165.70, 163.08, 148.60, 148.32, 147.55, 138.88, 138.16, 133.66, 133.45, 131.99, 131.37, 130.45, 130.22, 129.61, 129.58, 128.72, 126.69, 123.81, 122.70, 118.38, 114.42, 104.03, 72.89, 58.81, 55.72, 54.55, 53.78, 35.16, 27.30, 20.23, 18.01; LRMS-ESI (*m/z*): [M+H] 700.3. HRMS (ESI) *m/z*: [M+H] calcd $C_{37}H_{41}N_5O_5S_2H$ 700.262739; found 700.26288.

N-((2S,3R)-3-hydroxy-4-((N-isobutyl-4-methoxyphenyl)sulfonamido)-1-phenylbutan-2-yl)-2-methyl-3-((4-(pyridin-3-yl)thiazol-2-yl)amino)benzamide **(5f).** Inhibitor **5f** was synthesized according to the same procedure as inhibitor **5e** utilizing **19b** (14.0 mg, 0.05 mmol), CH_2Cl_2 (1.0 mL), triethylamine (0.04 mL, 0.27 mmol), HATU (22.0 mg, 0.06 mmol), and **11** (0.05 mmol). The crude product was purified via silica gel column chromatography (50-60% EtOAc/hexanes) to afford **5f** (16.7 mg, 53.9%): ^{1}H NMR (500 MHz, CD_3OD) δ 9.01 (s, 1H), 8.44 (d, *J* = 4.3 Hz, 1H), 8.26 (dt, *J* = 8.0, 1.6 Hz, 1H), 7.88 (d, *J* = 7.9 Hz, 1H), 7.78 (d, *J* = 8.9 Hz, 2H), 7.45 (dd, *J* = 8.0, 4.9 Hz, 1H), 7.33 – 7.23 (m, 4H), 7.24 – 7.16 (m, 3H), 7.06 (d, *J* = 8.9 Hz, 2H), 6.86 (d, *J* = 7.5 Hz, 1H), 4.34 – 4.29 (m, 1H), 3.94 – 3.86 (m, 1H), 3.84 (s, 3H), 3.60 (dd, *J* = 14.9, 2.9 Hz, 1H), 3.14 – 3.04 (m, 2H), 2.93 (dd, *J* = 13.6, 6.8 Hz, 1H), 2.82 (s, 1H), 2.65 (dd, *J* = 13.9, 11.8 Hz, 1H), 2.08 (dt, *J* = 14.2, 7.0 Hz, 1H), 1.90 (s, 3H), 0.92 (dd, *J* = 30.3, 6.6 Hz, 6H); ^{13}C NMR (125 MHz, CD_3OD) δ 172.75, 168.69, 164.55, 148.67, 148.64, 147.70, 141.13, 140.21, 139.89, 135.21, 132.73, 132.20, 130.64, 130.52, 129.38, 127.55, 127.36, 127.32, 125.28, 124.80, 123.94, 115.39, 105.60, 74.57, 58.93, 56.19, 55.63, 54.11, 36.88, 28.11, 20.56, 20.48, 14.72; LRMS-ESI (*m/z*): [M+H] 700.5. HRMS (ESI) *m/z*: [M+H] calcd $C_{37}H_{41}N_5O_5S_2H$ 700.262739; found 700.26285.

N-((2S,3R)-3-hydroxy-4-((N-isobutyl-4-methoxyphenyl)sulfonamido)-1-phenylbutan-2-yl)-3-methyl-5-((4-(pyridin-3-yl)thiazol-2-yl)amino)benzamide **(5g).** Inhibitor **5g** was synthesized according to the same procedure as inhibitor **5e** utilizing **19c** (23.0 mg, 0.07 mmol), CH_2Cl_2 (1.2 mL), triethylamine (0.06 mL, 0.1 mmol), HATU (36.0 mg, 0.1 mmol), and **11** (0.08 mmol). The crude product was purified via silica gel column chromatography (50-60% EtOAc/hexanes) to afford **5g** (11.2 mg, 22%): ^{1}H NMR (500 MHz, CD_3OD) δ 9.09 (d, *J* = 1.8 Hz, 1H), 8.44 (dd, *J* = 4.9, 1.6 Hz, 1H), 8.34 (dt, *J* = 8.0, 1.9 Hz, 1H), 8.18 (d, *J* = 9.2 Hz, 1H), 7.91 (s, 1H), 7.67 – 7.59 (m, 3H), 7.46 (ddd, *J* = 8.0, 4.9, 0.9 Hz, 1H), 7.31 – 7.26 (m, 3H), 7.21 (t, *J* = 7.6 Hz, 2H), 7.14 – 7.10 (m, 2H), 6.89 – 6.83 (m, 2H), 4.22 (d, *J* = 9.6 Hz, 1H), 3.99 (td, *J* = 8.3, 2.7 Hz, 1H), 3.72 (s, 3H), 3.41 (dd, *J* = 15.2, 2.7 Hz, 1H), 3.10 (dd, *J* = 13.5, 8.7 Hz, 1H), 2.92 (dd, *J* = 15.2, 8.7 Hz, 1H), 2.88 – 2.74 (m, 3H), 2.40 (s, 3H), 2.09 – 2.02 (m, 1H), 0.90 (dd, *J* = 38.4, 6.6 Hz, 8H); ^{13}C NMR (125 MHz, CD_3OD) δ 170.39, 165.74, 164.42, 148.84, 148.55, 147.67, 142.72, 140.37, 140.26, 136.85, 135.45, 132.72, 131.49, 130.61, 130.37, 129.29, 127.23, 125.40, 121.94, 121.85, 115.24, 114.79, 105.68, 74.78, 61.53, 59.28, 56.05, 54.59, 36.94, 28.02, 21.69, 20.50, 14.45; LRMS-ESI (*m/z*): [M+H] 700.5. HRMS (ESI) *m/z*: [M+H] calcd $C_{37}H_{41}N_5O_5S_2H$ 700.262739; found 700.26397.

N-((2S,3R)-3-hydroxy-4-((N-isobutyl-4-methoxyphenyl)sulfonamido)-1-phenylbutan-2-yl)-2-methyl-5-((4-(pyridin-3-yl)thiazol-2-yl)amino)benzamide **(5h).** Inhibitor **5h** was synthesized according to the same procedure as inhibitor **5e** utilizing **19d** (33.1 mg, 0.11 mmol), CH_2Cl_2 (1.8 mL), triethylamine (0.09 mL, 0.64 mmol), HATU (52.0 mg, 0.14 mmol), and **11** (0.12 mmol). The crude product was purified via silica gel column chromatography (60% EtOAc/hexanes) to afford **5h** (24.1 mg, 32%): ^{1}H NMR (500 MHz, $CDCl_3$) δ 9.12 (s, 1H), 8.47 (s, 1H), 8.01 (d, *J* = 7.8 Hz, 2H), 7.71 (d, *J* = 8.9 Hz, 2H), 7.61 (s, 1H), 7.27 (dt, *J* = 15.0, 7.4 Hz, 3H), 7.17 (dd, *J* = 15.3, 8.1 Hz, 2H), 7.04 (d, *J* = 8.3 Hz, 1H), 6.91 (d, *J* = 8.9 Hz, 2H), 6.84 (s, 1H), 6.51 (d, *J* = 9.0 Hz, 1H), 4.59 – 4.49 (m, 1H), 4.13 (td, *J* = 7.4, 3.7 Hz, 1H), 3.80 (s, 3H), 3.29 – 3.10 (m, 3H), 3.02 – 2.90 (m, 3H), 2.03 (s, 3H), 1.92 (tt, *J* = 14.9, 7.6 Hz, 1H), 0.89 (dd, *J* = 13.4, 6.6 Hz, 6H). ^{13}C NMR (125 MHz, $CDCl_3$) δ 169.94, 164.73, 163.05, 148.16, 147.88, 147.69, 138.20, 138.12, 136.87, 133.25, 131.83, 130.80, 130.48, 129.60, 128.66, 127.92, 126.64, 123.81, 119.87, 117.06, 114.43, 114.06, 103.61, 72.91, 58.61, 55.69, 53.72, 34.74, 29.84, 27.29, 20.25, 18.79; LRMS-ESI (*m/z*): [M+H] 700.5. HRMS (ESI) *m/z*: [M+H] calcd $C_{37}H_{41}N_5O_5S_2H$ 700.262739; found 700.26323.

N-((2S,3R)-3-hydroxy-4-((N-isobutyl-4-methoxyphenyl)sulfonamido)-1-phenylbutan-2-yl)-2,4-dimethyl-3-((4-(pyridin-3-yl)thiazol-2-yl)amino)benzamide **(5i).** Inhibitor **5i** was synthesized according to the same procedure as inhibitor **5e** utilizing **19e** (17.8 mg, 0.06 mmol), CH_2Cl_2 (0.9 mL), triethylamine (0.05 mL, 0.33 mmol), HATU (27.0 mg, 0.07 mmol), and **11** (0.06 mmol). The crude product was purified via silica gel column chromatography (2% MeOH/CH_2Cl_2) to afford **5i** (7.5 mg, 19%): ^{1}H NMR (800 MHz, $CDCl_3$) δ 8.80 (s, 1H), 8.37 (s, 1H), 8.01 (d, *J* = 7.8 Hz, 1H), 7.72 (d, *J* = 8.9 Hz, 2H), 7.29 (m, 4H), 7.21 (t, *J* = 7.1 Hz, 1H), 7.07 (d, *J* = 7.8 Hz, 1H), 6.96 (dd, *J* = 15.9, 8.3 Hz, 3H), 6.79 (d, *J* = 20.7 Hz, 1H), 6.74 (s, 1H), 4.46 – 4.36 (m, 1H), 4.08 – 4.00 (m, 1H), 3.86 (s, 3H), 3.26 – 3.12 (m, 3H), 3.02 (dd, *J* = 14.2, 10.3 Hz, 1H), 2.92 (ddd, *J* = 38.8, 13.4, 7.5 Hz, 2H), 2.28 (s, 3H), 2.16 (s, 3H), 1.91 (dt, *J* = 13.7, 6.9 Hz, 1H), 0.89 (dd, *J* = 27.0, 6.6 Hz, 6H); ^{13}C NMR (200 MHz, $CDCl_3$) δ 170.60, 170.40, 163.21, 148.06, 146.48, 139.16, 138.13, 137.70, 136.74, 135.02, 133.98, 130.77, 130.04, 129.61, 129.57, 128.86, 128.78, 127.94, 126.80, 126.61, 123.87, 114.54, 114.08, 103.67, 73.27, 59.07, 55.78, 54.56, 53.86, 35.06, 27.48, 20.28, 20.11, 18.57, 15.04; LRMS-ESI (*m/z*): [M+H] 714.3. HRMS (ESI) *m/z*: [M+H] calcd $C_{38}H_{43}N_5O_5S_2H$ 714.27839; found 714.27875.

N-((2S,3R)-3-hydroxy-4-((N-isobutyl-4-methoxyphenyl)sulfonamido)-1-phenylbutan-2-yl)-4-methyl-3-((4-methylthiazol-2-yl)amino)benzamide **(5j).** Inhibitor **5j** was synthesized according to the same procedure as inhibitor **5e** utilizing **21a** (17.0 mg, 0.05 mmol), CH_2Cl_2 (0.9 mL), triethylamine (0.05 mL, 0.33 mmol), HATU (27.0 mg, 0.07 mmol), and **11** (0.06 mmol). The crude product was purified via silica gel column chromatography (35% EtOAc/hexanes) to afford **5j** (13.2 mg, 38.8%): ^{1}H NMR (500 MHz, $CDCl_3$) δ 7.72 – 7.69 (m, 2H), 7.33 – 7.17 (m, 5H), 7.11 (d, *J* = 8.3 Hz, 1H), 7.01 (d, *J* = 2.5 Hz, 1H), 6.99 – 6.94 (m, 2H), 6.19 (s, 1H), 6.06 (d, *J* = 8.6 Hz, 1H), 4.41 – 4.35 (m, 1H), 4.20 (bs, 1H), 4.01 – 3.98 (m, 1H), 3.86 (s, 3H), 3.20 – 3.11 (m, 3H), 3.05 – 2.91 (m, 2H), 2.93 – 2.85 (m, 1H), 2.28 (s, 3H), 2.16 (s, 3H), 1.92 – 1.87 (m, 1H), 0.90 (dd, *J* = 17.6, 6.6 Hz, 6H); ^{13}C NMR (125 MHz, $CDCl_3$) δ 170.08, 164.33, 163.21, 148.96, 138.33, 137.90, 136.77, 132.17, 130.51, 130.01, 129.61, 129.55, 128.84, 126.84, 120.00, 116.83, 114.53, 102.42, 73.08, 59.07, 55.78, 54.38, 53.85, 35.15, 27.48, 20.27, 20.09, 18.97, 17.46; LRMS-ESI (*m/z*): [M+H] 637.2. HRMS (ESI) *m/z*: [M+H] calcd $C_{33}H_{40}N_4O_5S_2H$ 637.25184; found 637.25175.

N-((2S,3R)-3-hydroxy-4-((N-isobutyl-4-methoxyphenyl)sulfonamido)-1-phenylbutan-2-yl)-2-methyl-3-((4-methylthiazol-2-yl)amino)benzamide **(5k).** Inhibitor **5k** was synthesized according to the same procedure as inhibitor **5e** utilizing **21b** (20.1 mg, 0.08 mmol), CH_2Cl_2 (1.35 mL), triethylamine (0.07 mL, 0.49 mmol), HATU (40.0 mg, 0.11 mmol), and **11** (0.09 mmol). The crude product was purified via silica gel column chromatography (35% EtOAc/hexanes) to afford **5k** (13.2 mg, 25.3%): ^{1}H NMR (500 MHz, $CDCl_3$) δ 7.75 – 7.69 (m, 2H), 7.64 (d, *J* = 8.1 Hz, 1H), 7.32 – 7.27 (m, 3H), 7.25 – 7.22 (m, 1H), 7.15 (t, *J* = 7.9 Hz, 1H), 7.01 – 6.95 (m, 2H), 6.76 (dd, *J* = 7.6, 1.2 Hz, 1H), 6.17 (d, *J* = 1.3 Hz, 1H), 6.01 (d, *J* = 8.7 Hz, 1H), 4.39 (dd, *J* = 9.2, 4.8 Hz, 1H), 4.00 (dt, *J* = 7.5, 4.5 Hz, 1H), 3.87 (d, *J* = 1.6 Hz, 3H), 3.22 – 3.11 (m, 3H), 3.01 – 2.83 (m, 3H), 2.28 (d, *J* = 1.1 Hz, 3H), 2.04 (s, 3H), 1.95 – 1.87 (m, 1H), 0.96 – 0.86 (m, 6H); ^{13}C NMR (125 MHz, $CDCl_3$) δ 170.37, 165.60, 163.24, 139.67, 138.16, 137.85, 129.97, 129.61, 129.50, 128.83, 127.03, 126.88, 126.79, 126.63, 122.29, 121.59, 114.55, 102.54, 73.14, 59.08, 55.78, 54.36, 53.85, 35.18, 27.48, 20.28, 20.08, 17.29, 14.09; LRMS-ESI (*m/z*): [M+H] 637.2. HRMS (ESI) *m/z*: [M+H] calcd $C_{33}H_{40}N_4O_5S_2H$ 637.25184; found 637.25154.

N-((2S,3R)-3-hydroxy-4-((N-isobutyl-4-methoxyphenyl)sulfonamido)-1-phenylbutan-2-yl)-3-methyl-5-((4-methylthiazol-2-yl)amino)benzamide **(5l).** Inhibitor **5l** was synthesized according to the same procedure as inhibitor **5e** utilizing **21c** (28.4 mg, 0.09 mmol), CH_2Cl_2 (1.5 mL), triethylamine (0.07 mL, 0.52 mmol), HATU (43.0 mg, 0.11 mmol), and **11** (0.10 mmol). The crude product was purified via silica gel column chromatography (35% EtOAc/hexanes) to afford **5l** (10.2 mg, 18.5%): ^{1}H NMR (800 MHz, $CDCl_3$) δ 7.68 (dq, *J* = 9.0, 2.4, 1.6 Hz, 2H), 7.42 (s, 1H), 7.32 – 7.24 (m, 4H), 7.22 – 7.17 (m, 1H), 7.02 (s, 1H), 6.95 – 6.91 (m, 2H), 6.49 (d, *J* = 8.3 Hz, 1H), 6.21 (s, 1H), 4.39 (dq, *J* = 8.2, 3.0 Hz, 1H), 4.00 (dt, *J* = 8.4, 4.3 Hz, 1H), 3.84 (s, 3H), 3.19 (dd, *J* = 15.1, 4.1 Hz, 1H), 3.12– 3.08 (m, 3H), 2.88 (d, *J* = 7.5 Hz, 2H), 2.34 (s, 3H), 2.29 (s, 3H), 1.89 – 1.83 (m, 1H), 0.86 (dd, *J* = 9.7, 6.6 Hz, 6H); ^{13}C NMR (200 MHz, $CDCl_3$) δ 167.92, 164.05, 163.17, 147.93, 140.62, 140.18, 137.92, 135.50, 129.99, 129.59, 128.82, 126.82, 122.00, 121.67, 114.49, 113.83, 102.45, 72.94, 58.98, 55.75, 54.72, 53.68, 35.23, 27.37, 21.64, 20.24, 20.13, 17.14; LRMS-ESI (*m/z*): [M+H] 637.3. HRMS (ESI) *m/z*: [M+H] calcd $C_{33}H_{40}N_4O_5S_2H$ 637.25184; found 637.25228.

N-((2S,3R)-3-hydroxy-4-((N-isobutyl-4-methoxyphenyl)sulfonamido)-1-phenylbutan-2-yl)-2-methyl-5-((4-methylthiazol-2-yl)amino)benzamide **(5m).** Inhibitor **5m** was synthesized according to the same procedure as inhibitor **5e** utilizing **21d** (25.0 mg, 0.1 mmol), CH_2Cl_2 (0.17 mL), triethylamine (0.084 mL, 0.6 mmol), HATU (49.0 mg, 0.13 mmol), and **11** (0.11 mmol). The crude product was purified via silica gel column chromatography (35-40% EtOAc/hexanes) to afford **5m** (13.4 mg, 25.8%): ^{1}H NMR (500 MHz, $CDCl_3$) δ 7.74 – 7.66 (m, 2H), 7.33 – 7.17 (m, 5H), 7.11 (d, *J* = 8.2 Hz, 1H), 7.01 (d, *J* = 2.5 Hz, 1H), 6.99 – 6.93 (m, 2H), 6.19 (d, *J* = 1.2 Hz, 1H), 6.07 (d, *J* = 8.6 Hz, 1H), 4.37 (dq, *J* = 9.4, 4.6 Hz, 1H), 3.99 (dd, *J* = 7.4, 4.6 Hz, 1H), 3.86 (s, 3H), 3.22 – 3.09 (m, 3H), 3.06 – 2.82 (m, 3H), 2.28 (d, *J* = 1.1 Hz, 3H), 2.16 (s, 3H), 1.90 (dt, *J* = 13.8, 6.8 Hz, 1H), 0.90 (dd, *J* = 17.8, 6.6 Hz, 6H); ^{13}C NMR (125 MHz, $CDCl_3$) δ 170.07, 164.43, 163.21, 138.27, 137.91, 136.78, 132.18, 130.58, 130.01, 129.61, 129.55, 128.83, 126.84, 120.02, 116.84, 114.53, 102.35, 73.08, 59.07, 55.78, 54.38, 53.85, 35.15, 29.85, 27.48, 20.27, 20.09, 18.97, 17.39; LRMS-ESI (*m/z*): [M+H] 637.3. HRMS (ESI) *m/z*: [M+H] calcd $C_{33}H_{40}N_4O_5S_2H$ 637.25184; found 637.25186.

N-((2S,3R)-3-hydroxy-4-((N-isobutyl-4-methoxyphenyl)sulfonamido)-1-phenylbutan-2-yl)-4-methyl-3-((4-(trifluoromethyl)thiazol-2-yl)amino)benzamide **(5n).** Inhibitor **5n** was synthesized according to the same procedure as inhibitor **5e** utilizing **24a** (24.9 mg, 0.079 mmol), CH_2Cl_2 (1.0 mL), triethylamine (0.066 mL, 0.472 mmol), HATU (39.0 mg, 0.102 mmol), and **11** (0.094 mmol). The crude product was purified via silica gel column chromatography (50% EtOAc/hexanes) to afford **5n** (25.9 mg, 35%): ^{1}H NMR (500 MHz, $CDCl_3$) δ 7.89 (d, *J* = 1.8 Hz, 1H), 7.79 – 7.69 (m, 3H), 7.32 (dd, *J* = 9.9, 5.8 Hz, 7H), 7.12 – 6.96 (m, 3H), 6.57 (d, *J* = 8.3 Hz, 1H), 4.43 (dd, *J* = 7.9, 4.5 Hz, 1H), 4.09 – 4.03 (m, 1H), 3.90 (s, 3H), 3.30 – 3.10 (m, 4H), 2.92 (dd, *J* = 7.6, 3.0 Hz, 2H), 2.37 (s, 3H), 1.96 – 1.87 (m, 1H), 0.90 (s, 7H). ^{13}C NMR (126 MHz, $CDCl_3$) δ 167.96, 167.16, 163.07, 138.38, 137.82, 134.37, 133.41, 131.59, 129.90, 129.47, 129.43, 128.68, 126.68, 123.62, 121.39, 120.06, 119.24, 114.38, 109.74, 72.82, 58.82, 55.65, 54.67, 53.52, 45.95, 35.09, 30.98, 29.74, 27.25, 20.12,

20.01, 17.88, 8.64; LRMS-ESI (m/z): LRMS-ESI (*m/z*): [M+H] 691.2. HRMS (ESI) *m/z*: [M+H] calcd $C_{33}H_{37}F_3N_4O_5S_2H$ 691.22357; found 691.22424.

N-((2S,3R)-3-hydroxy-4-((N-isobutyl-4-methoxyphenyl)sulfonamido)-1-phenylbutan-2-yl)-2-methyl-3-((4-(trifluoromethyl)thiazol-2-yl)amino)benzamide **(5o).** Inhibitor **5o** was synthesized according to the same procedure as inhibitor **5e** utilizing **24b** (20.1 mg, 0.063 mmol), CH_2Cl_2 (1.0 mL), triethylamine (0.05 mL, 0.378 mmol), HATU (31.1 mg, 0.08 mmol), and **11** (0.08 mmol). The crude product was purified via silica gel column chromatography (50% EtOAc/hexanes) to afford **5o** (15.4 mg, 35.4%): ^{1}H NMR (500 MHz, $CDCl_3$) δ 7.76 – 7.68 (m, 2H), 7.56 – 7.44 (m, 1H), 7.30 (d, *J* = 6.3 Hz, 4H), 7.25 – 7.16 (m, 2H), 7.03 – 6.94 (m, 3H), 6.89 (dd, *J* = 8.1, 2.0 Hz, 1H), 6.10 (dd, *J* = 18.5, 8.8 Hz, 1H), 4.42 (s, 1H), 3.87 (s, 3H), 3.16 (ddd, *J* = 14.6, 8.7, 5.8 Hz, 3H), 3.00 – 2.93 (m, 2H), 2.91 – 2.84 (m, 1H), 2.05 (d, *J* = 10.2 Hz, 3H), 1.91 (t, *J* = 7.0 Hz, 1H), 0.91 (dd, *J* = 14.3, 6.5 Hz, 6H); ^{13}C NMR (126 MHz, $CDCl_3$) δ 172.15, 171.31, 163.53, 137.95, 137.60, 136.98, 131.81, 131.54, 129.59, 129.33, 129.18, 129.02, 127.85, 127.27, 126.56, 126.29, 126.00, 114.70, 73.04, 58.97, 55.81, 54.60, 53.57, 53.11, 34.51, 31.09, 29.85, 27.44, 26.92, 20.15, 19.89, 19.46, 14.23. LRMS-ESI (*m/z*): [M+H] 691.2. HRMS (ESI) *m/z*: [M+H] calcd $C_{33}H_{37}F_3N_4O_5S_2H$ 691.22357; found 691.22400.

N-((2S,3R)-3-hydroxy-4-((N-isobutyl-4-methoxyphenyl)sulfonamido)-1-phenylbutan-2-yl)-5-((4-(methoxymethyl)thiazol-2-yl)amino)-2-methylbenzamide **(5p).** Inhibitor **5p** was synthesized according to the same procedure as inhibitor **5e** utilizing **27** (17.4 mg, 0.06 mmol), CH_2Cl_2 (1.1 mL), triethylamine (0.05 mL, 0.38 mmol), HATU (31.0 mg, 0.08 mmol), and **11** (0.07 mmol). The crude product was purified via silica gel column chromatography (35% EtOAc/hexanes) to afford **5p** (10.6 mg, 25.2%): ^{1}H NMR (800 MHz, $CDCl_3$) δ 7.71 (d, *J* = 8.8 Hz, 2H), 7.31 – 7.27 (m, 3H), 7.24 – 7.19 (m, 2H), 7.12 (d, *J* = 8.1 Hz, 2H), 6.98 – 6.96 (m, 3H), 6.53 (s, 1H), 6.07 (d, *J* = 8.7 Hz, 1H), 4.40 (s, 2H), 4.18 (s, 1H), 4.01 (d, *J* = 6.1 Hz, 1H), 3.87 (s, 3H), 3.44 (s, 3H), 3.18 – 3.14 (m, 3H), 3.01 (dd, *J* = 14.3, 10.0 Hz, 1H), 2.96 – 2.93 (m, 1H), 2.88 (d, *J* = 6.4 Hz, 1H), 2.17 (s, 3H), 1.90 (dt, *J* = 14.0, 6.8 Hz, 1H), 0.90 (dd, *J* = 26.3, 6.6 Hz, 6H); ^{13}C NMR (200 MHz, $CDCl_3$) δ 169.96, 163.22, 138.07, 137.93, 136.87, 132.26, 130.04, 129.62, 129.55, 129.37, 128.85, 127.95, 126.85, 120.24, 117.16, 114.54, 114.08, 105.18, 73.09, 70.53, 59.06, 58.71, 55.79, 54.37, 53.83, 35.08, 27.48, 20.28, 20.10, 19.00; LRMS-ESI (*m/z*): [M+H] 667.2. HRMS (ESI) *m/z*: [M+H] calcd $C_{34}H_{42}N_4O_6S_2H$ 667.26241; found 667.26216.

Methyl 3-(3-acetylthioureido)-4-methylbenzoate **(16a).** To a solution of potassium thiocyanate (292 mg, 3.0 mmol) in acetone (7.5 mL) was added acetyl chloride (0.14 mL, 2.0 mmol) dropwise. The reaction mixture was stirred at 60 °C for 1.5 h. To the reaction was then added methyl 3-amino-4-methylbenzoate (165 mg, 1.0 mmol) and the reaction was stirred at 23 °C for 4 h. The reaction was then filtered and concentrated under reduced pressure. The crude product was purified via silica gel column chromatography (25% ethyl acetate/hexanes) to afford the desired thiourea in quantitative yield as a white solid: ^{1}H NMR (500 MHz, CD_3OD) δ 8.27 (d, *J* = 1.8 Hz, 1H), 7.85 (dd, *J* = 8.0, 1.8 Hz, 1H), 7.39 (d, *J* = 8.0 Hz, 1H), 3.90 (d, *J* = 0.8 Hz, 3H), 2.33 (s, 3H), 2.19 (d, *J* = 0.8 Hz, 3H); ^{13}C NMR (125 MHz, $CDCl_3$) δ 181.89, 173.93, 173.15, 168.03, 140.84, 138.52, 131.82, 129.59, 129.01, 52.64, 23.87, 18.30.

Methyl 3-(3-acetylthioureido)-2-methylbenzoate **(16b).** Thiourea **16b** was synthesized according to the same procedure as thiourea **16a** utilizing potassium thiocyanate (292 mg, 3.0 mmol), acetone (7.5 mL), acetyl chloride (0.14 mL, 2.0 mmol), methyl 3-amino-2-methylbenzoate (165 mg, 1.0 mmol). The crude mixture was purified via silica gel column chromatography (25% ethyl acetate/hexanes) to afford the desired thiourea in quantitative yield as a white solid: ^{1}H NMR (500 MHz, $CDCl_3$) δ 9.39 (s, 1H), 7.85 (d, *J* = 7.7 Hz, 1H), 7.69 (d, *J* = 7.8 Hz, 1H), 7.31 (t, *J* = 7.9 Hz, 1H), 3.90 (s, 3H), 2.50 (s, 3H), 2.22 (s, 3H); ^{13}C NMR (125 MHz, $CDCl_3$) δ 180.24, 171.67, 167.91, 137.46, 135.87, 131.83, 130.97, 130.17, 126.04, 52.29, 24.56, 15.37.

Methyl 3-(3-acetylthioureido)-5-methylbenzoate **(16c).** Thiourea **16c** was synthesized according to the same procedure as thiourea **16a** utilizing potassium thiocyanate (292 mg, 3.0 mmol), acetone (7.5 mL), acetyl chloride (0.14 mL, 2.0 mmol), methyl 3-amino-2-methylbenzoate (165 mg, 1.0 mmol). The crude mixture was purified via silica gel column chromatography (25% ethyl acetate/hexanes) to afford methyl 3-(3-acetylthioureido)-5-methylbenzoate (138 mg, 42.5%): ^{1}H NMR (500 MHz, $CDCl_3$) δ 12.31 (s, 1H), 8.90 (s, 1H), 3.91 (s, 3H), 2.42 (2, 3H), 2.22 (s, 3H); ^{13}C NMR (125 MHz, $CDCl_3$) δ 178.71, 171.20, 166.60, 139.36, 137.69, 131.01, 129.41, 128.89, 122.81, 52.42, 24.66, 21.44.

Methyl 5-(3-acetylthioureido)-2-methylbenzoate **(16d).** Thiourea **16d** was synthesized according to the same procedure as thiourea **16a** utilizing potassium thiocyanate (353 mg, 3.6 mmol), acetone (9 mL), acetyl chloride (0.17 mL, 2.4 mmol), 5-amino-2-methylbenzoate (200 mg, 1.2 mmol). The crude mixture was purified via silica gel column chromatography (25% ethyl acetate/hexanes) to afford methyl 5-(3-acetylthioureido)-2-methylbenzoate (181 mg, 56%): ^{1}H NMR (500 MHz, $CDCl_3$) δ 8.87 (s, 1H), 8.08 (d, *J* = 2.2 Hz, 1H), 7.76 (dd, *J* = 8.3, 2.3 Hz, 1H), 7.28 (d, *J* = 8.3 Hz, 1H), 3.90 (s, 3H), 2.60 (s, 3H), 2.22 (s, 3H); ^{13}C NMR (125 MHz, $CDCl_3$) δ 178.74, 171.18, 167.24, 139.40, 135.31, 132.35, 130.04, 128.05, 126.67, 52.18, 24.66, 21.57.

Methyl 3-(3-acetylthioureido)-2,4-dimethylbenzoate **(16e).** Thiourea **16e** was synthesized according to the same procedure as thiourea **16a** utilizing potassium thiocyanate (33 mg, 0.34 mmol), acetone (0.84 mL), acetyl chloride (0.02 mL, 0.22 mmol), and methyl 3-amino-2,4-dimethylbenzoate (0.02 mg, 0.11 mmol). The crude product was purified *via* silica gel column chromatography (30% ethyl acetate/hexanes) to afford methyl 3-(3-acetylthioureido)-2,4-methylbenzoate (26.7 mg, 85%): ^{1}H NMR (500 MHz, $CDCl_3$) δ 9.91 (s, 1H), 7.82 (d, *J* = 8.0 Hz, 1H), 7.17 (d, *J* = 8.1 Hz, 1H), 3.88 (s, 3H), 2.48 (s, 3H), 2.31 (s, 3H), 2.22 (s, 3H); ^{13}C NMR (125 MHz, $CDCl_3$) δ 180.55, 172.07, 167.86, 140.28, 137.77, 136.42, 130.64, 129.18, 127.95, 52.09, 24.43, 18.90, 15.67; LRMS-ESI (*m/z*): $[M+H]^+$ 281.0.

Methyl 4-methyl-3-((4-(pyridin-3-yl)thiazol-2-yl)amino)benzoate **(18a).** To a stirring solution of **16a** (58 mg, 0.22 mmol) in dry methanol (1.3 mL) was added K_2CO_3 (182 mg, 1.32 mmol) and stirred for 5 minutes. To the reaction was then added 3-(bromoacetyl)pyridine•HBr (62 mg, 0.22 mmol) and the reaction was stirred for 6 h. The reaction mixture was then concentrated under reduced pressure and diluted with ethyl acetate and water. The aqueous layer was extracted with ethyl acetate (3x) and the combined organic layers were washed with brine, dried over Na_2SO_4, filtered, and concentrated under reduced pressure. The crude product was purified via silica gel column chromatography (50% ethyl acetate/hexanes) to afford **18a** as a white solid (45 mg, 60%): ^{1}H NMR (500 MHz, $CDCl_3$) δ 9.14 (d, *J* = 2.3 Hz, 1H), 8.55 – 8.47 (m, 2H), 8.11 (dt, *J* = 7.9, 2.0 Hz, 1H), 7.76 (dd, *J* = 7.9, 1.7 Hz, 1H), 7.59 – 7.51 (bs, 1H), 7.32 – 7.27 (m, 2H), 6.91 (s, 1H), 3.93 (s, 3H), 2.39 (s, 3H); ^{13}C NMR (125 MHz, $CDCl_3$) δ 166.82, 166.18, 148.83, 148.60, 147.68, 138.90, 134.34, 133.43, 131.26, 130.53, 129.51, 125.63, 123.62, 121.52, 103.72, 52.36, 18.24; LRMS-ESI (*m/z*): $[M+H]^+$ 326.1.

Methyl 4-methyl-3-((4-(pyridin-3-yl)thiazol-2-yl)amino)benzoate **(18b).** Thiazole **18b** was synthesized according to the same procedure as thiazole **18a** utilizing **16b** (77.7 mg, 0.29 mmol), methanol (1 mL), K_2CO_3 (242 mg, 1.75 mmol), and 3-(bromoacetyl)pyridine•HBr (82 mg, 0.29 mmol). The crude product was then purified via silica gel column chromatography (50% ethyl acetate/hexanes) to afford **18b** as a white solid (58 mg, 61%): ^{1}H NMR (500 MHz, $CDCl_3$) δ 9.29 (s, 1H), 8.64 (bs, 1H), 8.52 (d, *J* = 4.0

Hz, 1H), 8.07 (dt, *J* = 7.9, 1.7 Hz, 1H), 7.87 (d, *J* = 7.4 Hz, 1H), 7.73 (d, *J* = 7.7 Hz, 1H), 7.33 (t, *J* = 7.9 Hz, 1H), 7.28 (dd, *J* = 7.8, 4.8 Hz, 1H), 6.87 (s, 1H), 3.95 (s, 3H), 2.57 (s, 3H); ^{13}C NMR (125 MHz, $CDCl_3$) δ 168.27, 168.11, 148.53, 148.40, 147.64, 140.12, 133.29, 132.76, 132.29, 130.59, 127.34, 126.66, 126.62, 123.44, 103.29, 52.22, 15.01; LRMS-ESI (*m/z*): $[M+H]^+$ 326.1.

Methyl 3-methyl-5-((4-(pyridin-3-yl)thiazol-2-yl)amino)benzoate **(18c).** Thiazole **18c** was synthesized according to the same procedure as thiazole **18a** utilizing **16c** (57 mg, 0.215 mmol), methanol (0.77 mL), K_2CO_3 (178 mg, 1.29 mmol), and 3-(bromoacetyl)pyridine•HBr (60 mg, 0.215 mmol). The crude product was purified via silica gel column chromatography (50% EtOAc/hexanes) to afford **17c** (60 mg, 86%): ^{1}H NMR (500 MHz, $CDCl_3$) δ 9.21 – 9.15 (m, 1H), 8.56 (d, *J* = 4.9 Hz, 1H), 8.17 (dt, *J* = 8.1, 1.9 Hz, 1H), 7.96 (s, 1H), 7.57 (s, 1H), 7.51 (s, 1H), 7.37 (dd, *J* = 8.0, 4.8 Hz, 1H), 6.96 (s, 1H), 3.93 (s, 3H), 2.42 (s, 3H); ^{13}C NMR (125 MHz, $CDCl_3$) δ 167.01, 164.66, 148.28, 147.27, 140.51, 139.89, 133.87, 131.38, 130.72, 124.95, 123.86, 123.13, 116.37, 113.27, 103.79, 52.44, 21.68; LRMS-ESI (*m/z*): $[M+H]^+$ 326.1.

Methyl 2-methyl-5-((4-(pyridin-3-yl)thiazol-2-yl)amino)benzoate **(18d).** Thiazole **18d** was synthesized according to the same procedure as thiazole **18a** utilizing **16d** (24 mg, 0.09 mmol), methanol (0.32 mL), K_2CO_3 (75 mg, 0.54 mmol), 3-(bromoacetyl)pyridine•HBr (25 mg, 0.09 mmol). The crude product was purified via silica gel column chromatography (50% ethyl acetate/hexanes) to afford **17d** (65 mg, 66%): ^{1}H NMR (500 MHz, $CDCl_3$) δ 9.14 (d, *J* = 1.6 Hz, 1H), 8.56 (d, *J* = 6.3 Hz, 1H), 8.21 (dt, *J* = 7.9, 1.7 Hz, 1H), 8.06 (d, *J* = 2.5 Hz, 1H), 7.56 (dd, *J* = 8.2, 2.6 Hz, 1H), 7.41 (dd, *J* = 7.8, 5.0 Hz, 1H), 7.26 (d, *J* = 8.2 Hz, 3H), 6.95 (s, 1H), 3.93 (s, 3H), 2.58 (s, 3H); ^{13}C NMR (125 MHz, $CDCl_3$) δ 167.66, 165.14, 147.50, 146.52, 138.05, 135.32, 134.49, 132.96, 130.42, 128.73, 127.39, 124.10, 122.24, 120.78, 103.94, 52.21, 21.28; LRMS-ESI (*m/z*): $[M+H]^+$ 326.2.

Methyl 2,4-dimethyl-3-((4-(pyridin-3-yl)thiazol-2-yl)amino)benzoate **(18e).** Thiazole **18e** was synthesized according to the same procedure as thiazole **18a** utilizing **16e** (12.7 mg, 0.05 mmol), methanol (0.28 mL), K_2CO_3 (0.04 mg, 0.27 mmol), 3-(bromoacetyl)pyridine•HBr (0.01 mg, 0.05 mmol. The crude product was purified *via* silica gel column chromatography (50% ethyl acetate/hexanes) to afford **17e** (12 mg, 78.4%): ^{1}H NMR (500 MHz, $CDCl_3$) δ 9.07 (d, *J* = 2.0 Hz, 1H), 8.50 (dd, *J* = 4.8, 1.4 Hz, 1H), 8.05 (dt, *J* = 7.9, 1.9 Hz, 1H), 7.82 (d, *J* = 8.0 Hz, 1H), 7.22 (d, *J* = 8.1 Hz, 1H), 6.77 (s, 1H), 3.90 (s, 3H), 2.58 (s, 3H), 2.38 (s, 3H); ^{13}C NMR (125 MHz, $CDCl_3$) δ 170.52, 167.98, 149.03, 148.44, 148.00, 147.03, 141.81, 139.24, 138.27, 133.86, 130.37, 130.02, 128.60, 123.76, 103.41, 52.20, 19.01, 15.76; LRMS-ESI (*m/z*): $[M+H]^+$ 340.1.

Methyl 4-methyl-3-((4-methylthiazol-2-yl)amino)benzoate **(20a).** To a stirring solution of chloroacetone (0.1 mL, 1.2 mmol) and KSCN (175 mg, 1.8 mmol) at 23 °C in dry methanol (0.8 mL) was stirred for 1 h. To the reaction was then added methyl 3-amino-4methylbenzoate (200 mg, 1.2 mmol) and stirred at 60 °C for 5 h. The reaction was then cooled to 23 °C, filtered and concentrated under reduced pressure. The crude product was purified *via* silica gel column chromatography (25% ethyl acetate/hexanes) to afford methyl **20a** (55 mg, 17.5%): ^{1}H NMR (500 MHz, $CDCl_3$) δ 8.24 (s, 1H), 7.74 (d, *J* = 6.4 Hz, 1H), 7.30 (d, *J* = 7.9 Hz, 1H), 6.20 (s, 1H), 3.91 (s, 3H), 2.37 (s, 3H), 2.31 (s, 3H); ^{13}C NMR (125 MHz, $CDCl_3$) δ 166.61, 165.91, 146.99, 138.49, 134.55, 131.26, 129.45, 125.71, 120.77, 102.19, 52.24, 18.16, 16.76; LRMS-ESI (*m/z*): $[M+H]^+$ 263.0.

Methyl 2-methyl-3-((4-methylthiazol-2-yl)amino)benzoate **(20b).** Thiazole **20b** was synthesized according to the same procedure as thiazole **20a** utilizing chloroacetone (0.1 mL, 1.2 mmol), KSCN (175 mg, 1.8 mmol), methanol (0.8 mL), and methyl 3-amino-2-methylbenzoate (200 mg, 1.2 mmol). The crude product was purified via silica gel column chromatography (25% EtOAc/hexanes) to afford methyl **20b** (100 mg, 32%): ^{1}H NMR (500 MHz, $CDCl_3$) δ 7.75 (dd, *J* = 8.0, 1.8 Hz, 1H), 7.63 (dd, *J* = 7.8, 1.4 Hz, 1H), 7.33 – 7.17 (m, 1H), 6.14 (dt, *J* = 2.8, 1.1 Hz, 1H), 3.90 (d, *J* = 0.9 Hz, 3H), 2.50 (s, 3H), 2.25 (dd, *J* = 3.1, 1.2 Hz, 3H); ^{13}C NMR (125 MHz, $CDCl_3$) δ 168.45, 166.98, 148.90, 140.13, 132.37, 131.70, 126.81, 126.65, 125.38, 102.30, 52.28, 17.38, 14.89; LRMS-ESI (*m/z*): $[M+H]^+$ 263.2.

Methyl 3-methyl-5-((4-methylthiazol-2-yl)amino)benzoate **(20c).** Thiazole **20c** was synthesized according to the same procedure as thiazole **20a** utilizing chloroacetone (0.05 mL, 0.61 mmol), KSCN (90 mg, 0.92 mmol), methanol (0.41 mL), methyl 3-amino-5-methylbenzoate (100 mg, 0.61 mmol). The crude product was purified via silica gel column chromatography (25% EtOAc/hexanes) to afford **20c** (110 mg, 69%): ^{1}H NMR (500 MHz, $CDCl_3$) δ 7.80 (s, 1H), 7.53 (s, 1H), 7.40 (s, 1H), 6.19 (s, 1H), 3.90 (s, 3H), 2.37 (s, 3H), 2.30 (s, 3H); ^{13}C NMR (125 MHz, $CDCl_3$) δ 167.04, 165.14, 148.55, 141.04, 139.67, 131.22, 124.62, 123.37, 116.68, 102.11, 52.28, 21.50, 17.41; LRMS-ESI (*m/z*): [M+H] 263.1.

Methyl 2-methyl-5-((4-methylthiazol-2-yl)amino)benzoate **(20d).** Thiazole **20d** was synthesized according to the same procedure as thiazole **20a** utilizing chloroacetone (0.05 mL, 0.61 mmol), KSCN (90 mg, 0.92 mmol), methanol (0.41 mL), and methyl 3-amino-5-methylbenzoate (100 mg, 0.61 mmol). The crude product was purified via silica gel column chromatography (25% EtOAc/hexanes) to afford **20d** (94 mg, 59%): ^{1}H NMR (500 MHz, $CDCl_3$) δ 7.87 (d, *J* = 2.6 Hz, 1H), 7.44 (dd, *J* = 8.2, 2.6 Hz, 1H), 7.20 (d, *J* = 8.3 Hz, 1H), 6.14 (s, 1H), 3.88 (s, 3H), 2.55 (s, 3H), 2.26 (s, 3H); ^{13}C NMR (125 MHz, $CDCl_3$) δ 167.68, 166.06, 148.49, 138.75, 134.93, 132.77, 130.29, 122.78, 121.44, 101.60, 52.01, 21.17, 17.42; LRMS-ESI (*m/z*): [M+H] 263.1.

Methyl 4-methyl-3-((4-(trifluoromethyl)thiazol-2-yl)amino)benzoate **(23a).** Thiazole **23a** was synthesized according to the same procedure as thiazole **18a** utilizing **16a** (150 mg, 0.636 mmol), methanol (3.25 mL), K_2CO_3 (528 mg, 3.816 mmol), 3-Bromo-1,1,1-trifluoroacetone (134 mg, 0.699 mmol). The crude product was purified via silica gel column chromatography (50% ethyl acetate/hexanes) to afford **23a** (141 mg, 60 % yield): ^{1}H NMR (500 MHz, $CDCl_3$) δ 8.27 (s, 1H), 8.17 (d, *J* = 1.7 Hz, 1H), 7.85 (dd, *J* = 7.9, 1.7 Hz, 1H), 7.36 (d, *J* = 7.9 Hz, 1H), 6.97 (s, 1H), 3.91 (s, 3H), 2.37 (s, 3H); ^{13}C NMR (126 MHz, $CDCl_3$) δ 169.53, 166.52, 141.01, 140.72, 138.41, 137.62, 131.62, 129.75, 127.51, 124.33, 121.42, 119.27, 109.39, 109.35, 52.38, 18.08. $[M+H]^+$ = 317.2.

Methyl 2-methyl-3-((4-(trifluoromethyl)thiazol-2-yl)amino)benzoate **(23b).** Thiazole **23b** was synthesized according to the same procedure as thiazole **18a** utilizing **16b** (90 mg, 0.338 mmol), methanol (1.20 mL), K_2CO_3 (280 mg, 2.025 mmol), 3-Bromo-1,1,1-trifluoroacetone (71 mg, 0.372 mmol). The crude product was purified via silica gel column chromatography (50% ethyl acetate/hexanes) to afford **23b** (75.9 mg, 71 % yield): ^{1}H NMR (400 MHz, $CDCl_3$) δ 7.79 (dd, *J* = 7.9, 1.3 Hz, 1H), 7.64 (dd, *J* = 7.9, 1.4 Hz, 1H), 7.33 (td, *J* = 7.9, 0.7 Hz, 1H), 6.96 (d, *J* = 1.2 Hz, 1H), 3.93 – 3.90 (m, 3H), 2.53 (s, 3H); ^{13}C NMR (101 MHz, $CDCl_3$) δ 170.33, 167.98, 138.95, 134.64, 132.73, 129.18, 127.93, 127.06, 121.35, 118.67, 109.25, 52.39, 15.09. LRMS-ESI (m/z): $[M+H]^+$ 317.1.

Methyl 5-((4-(methoxymethyl)thiazol-2-yl)amino)-2-methylbenzoate **(26).** Thiazole **26** was synthesized according to the same procedure as thiazole **18a** utilizing **16d** (12 mg, 0.05 mmol), methanol (0.45 mL), K_2CO_3 (6 mg mg, 0.05 mmol), and 1-bromo-3-methoxypropan-2-one (9 mg, 0.05 mmol). The crude product was purified via silica gel column chromatography (20% EtOAc/hexanes) to afford **26** (6 mg, 42%): ^{1}H NMR (500 MHz, $CDCl_3$) δ 7.84 (d, *J* = 2.6 Hz, 1H), 7.44 (dd, *J* = 8.3, 2.6 Hz, 1H), 7.22 (d, *J* = 8.3 Hz, 1H), 6.52 (s, 1H), 4.39 (s, 2H), 3.89 (s, 3H), 3.43 (s, 3H), 2.56 (s, 3H); ^{13}C

NMR (125 MHz, $CDCl_3$) δ 167.66, 165.85, 149.51, 138.24, 135.28, 132.93, 130.46, 122.65, 121.04, 104.85, 70.51, 58.67, 52.14, 21.23; LRMS-ESI (*m/z*): $[M+H]^+$ 293.1, $[M+Na]^+$ 315.0.

4-Methyl-3-((4-(pyridin-3-yl)thiazol-2-yl)amino)benzoic acid **(19a).** To a stirring solution of **18a** (0.028g, 0.086 mmol) in 1 M LiOH (0.15 mL) was added a few drops of methanol and THF. The reaction was stirred until completion, and then the organic solvent was evaporated under reduced pressure. The aqueous layer was acidified to pH 3-5 utilizing 10% citric acid. The precipitate was collected via filtration and used without further purification.

2-Methyl-3-((4-(pyridin-3-yl)thiazol-2-yl)amino)benzoic acid **(19b).** Carboxylic acid **18b** was synthesized according to the same procedure as carboxylic acid **19a** utilizing **18b** (53 mg, 0.16 mmol) and 1 M LiOH (0.5 mL).

3-Methyl-5-((4-(pyridin-3-yl)thiazol-2-yl)amino)benzoic acid **(19c).** Carboxylic acid **19c** was synthesized according to the same procedure as carboxylic acid **19a** utilizing **18c** (0.02 g, 0.062 mmol) and 1 M LiOH (0.15 mL).

2-Methyl-5-((4-(pyridin-3-yl)thiazol-2-yl)amino)benzoic acid **(19d).** Carboxylic acid **19d** was synthesized according to the same procedure as carboxylic acid **19a** utilizing **18d** (0.03 g, 0.09 mmol) and 1 M LiOH (0.28).

2,4-Dimethyl-3-((4-(pyridin-3-yl)thiazol-2-yl)amino)benzoic acid **(19e).** Carboxylic acid **19e** was synthesized according to the same procedure as carboxylic acid **19a** utilizing **18e** (13 mg, 0.04 mmol) and 1 M LiOH (0.08).

4-Methyl-3-((4-methylthiazol-2-yl)amino)benzoic acid **(21a).** Carboxylic acid **21a** was synthesized according to the same procedure as carboxylic acid **19a** utilizing **20a** (0.05 mg, 0.18 mmol) and 1 M LiOH (0.55 mL).

3-Methyl-5-((4-methylthiazol-2-yl)amino)benzoic acid **(21b).** Carboxylic acid **21b** was synthesized according to the same procedure as carboxylic acid **19a** utilizing **20b** (51.0 mg, 0.19 mmol) and 1 M LiOH (0.38 mL).

2-Methyl-3-((4-methylthiazol-2-yl)amino)benzoic acid **(21c).** Carboxylic acid **21c** was synthesized according to the same procedure as carboxylic acid **19a** utilizing **20c** (19.4 mg, 0.074 mmol) and 1 M LiOH (0.15 mL).

2-Methyl-5-((4-methylthiazol-2-yl)amino)benzoic acid **(21d).** Carboxylic acid **21d** was synthesized according to the same procedure as carboxylic acid **19a** utilizing **20d** (28.1 mg, 0.11 mmol) and 1 M LiOH (0.2 mL).

4-Methyl-3-((4-(trifluoromethyl)thiazol-2-yl)amino)benzoic acid **(24a).** Carboxylic acid **24a** was synthesized according to the same procedure as carboxylic acid **19a** utilizing **23a** (0.280 g, 0.885 mmol) and 1 M LiOH (1.95 mL).

2-Methyl-3-((4-(trifluoromethyl)thiazol-2-yl)amino)benzoic acid **(24b).** Carboxylic acid **24b** was synthesized according to the same procedure as carboxylic acid **19a** utilizing **23b** (0.40 g, 0.127 mmol) and 1 M LiOH (1.55 mL).

5-((4-(Methoxymethyl)thiazol-2-yl)amino)-2-methylbenzoic acid **(27).** Carboxylic acid **27** was synthesized according to the same procedure as carboxylic acid **19a** utilizing **26** (22.0 mg, 0.08 mmol) and 1 M LiOH (0.23 mL).

Determination of X-ray structure of HIV-1 protease-inhibitor complex

HIV-1 protease was expressed and purified as described previously.[54] Both protease complexes were crystallized by the hanging drop vapor diffusion method with well solution of 1.1 M NaCl, 0.1 M Sodium Acetate, pH 5.4 for PR/**5b** and 0.57 M NaCl, 0.1 M Sodium Acetate, pH 6.0 for PR/**5c**, respectively. Diffraction data were collected on a single crystal cooled to 90 K at SER-CAT (22-ID beamline), Advanced Photon Source, Argonne National Lab (Chicago, USA) with X-ray wavelength of 1.0 Å. The diffraction data were processed by HKL-2000,[55] to Rmerge of 10.4% in PR/**5b** and 6.2% in PR/**5c**, respectively. Both structures were solved by PHASER[56] in CCP4i Suite,[57,58,59] using the previously reported isomorphous structure with PDB code 3NU3[60] as the initial model. Both complexes were refined with REFMAC5.[61] Jligand[62] was used to construct the restraints for refinement. COOT[63,64] was used for model building. Anisotropic atomic displacement parameters (B factors) were applied for all atoms including solvent molecules. The final refined solvent structures comprised two Na^+ ions, four Cl^- ions, one acetate ion, one glycerol, one formic acid and 250 water molecules for PR/**5b** and one Na^+ ions, four Cl^- ions, one glycerol, two formic acid and 312 water molecules for PR/**5c**, respectively. The crystallographic statistics are listed in Table S1 (Please see supporting information). The coordinates and structure factors of both PR/GRL-02519A and PR/GRL-03419A were deposited in the Protein Data Bank[65] with code 8FUI and 8FUJ, respectively.

Declaration of competing interest

The authors declare that they have no known competing financial interests or personal relationships that could have appeared to influence the work reported in this paper.

Data Availability

Data will be made available upon request.

Acknowledgements

This research was supported by the National Institutes of Health (Grant AI150466, AKG and Grant AI150461, ITW). X-ray data were collected at the Southeast Regional Collaborative Access Team (SER-CAT) beamline 22BM at the Advanced Photon Source, Argonne National Laboratory. Use of the Advanced Photon Source was supported by the US Department of Energy, Basic Energy Sciences, Office of Science, under Contract No. W-31-109-Eng-38. This work was also supported by the Intramural Research Program of the Center for Cancer Research, National Cancer Institute, National Institutes of Health (HM), and in part by grants for the promotion of AIDS research from the Ministry of Health; grants from Welfare and Labor of Japan (HM); grants for the Research Program on HIV/AIDS from the Japan Agency for Medical Research and Development (AMED) under grant numbers JP15fk0410001 and JP16fk041001 (HM); a grant from the National Center for Global Health and Medicine (NCGM) Research Institute (HM); and a Grant-in-Aid for Scientific Research and a Grant-in-Aid for Challenging Research from the Ministry of Education, Culture, Sports, Science, and Technology of Japan (Monbu Kagakusho)(HM). The authors would like to thank the Purdue University Center for Cancer Research, which supports the shared NMR and mass spectrometry facilities.

ABBREVIATIONS USED: ART, antiretroviral therapies; *bis*-THF, *bis*-tetrahydrofuran; CML, chronic myeloid leukemia; CNS, central nervous system; DRV, darunavir; PR, protease ; PDB, Protein Data Bank

5. References and notes

1. 'Protease Inhibitors in AIDS Therapy' Ed. R. C. Ogden, C. W. Flexner, Marcel Dekker, New York **2011**, 1-300.

2. A. K. Ghosh, H. L. Osswald, G. Prato. Recent Progress in the Development of HIV-1 Protease Inhibitors for the Treatment of HIV/AIDS. *J. Med. Chem*. **2016**, *59*, 5172-5208.
3. J. A. Esté, T. C. Cihlar. Current status and challenges of antiretroviral research and therapy. *Antivir. Res.* **2010**, *85*, 25-33.
4. A. Wlodawer, J. Vondrasek. Inhibitors of HIV-1 protease: A major success of structure-assisted drug design. *Annu. Rev. Biophys Biomol. Struct.* **1998**, *27*, 249-284.
5. K. Appelt. Crystal structures of HIV-1 protease-inhibitor complexes. *Perspect. Drug Discov. Des.* **1993**, *1*, 23-48.
6. J. Maenza, C. Flexner, Combination Antiretroviral Therapy for HIV Infection. *Am. Fam. Physician*. **1998**, *57*, 2789-2798.
7. M. Vitoria, A. Rangaraj, N. Ford, M. Doherty. Current and future priorities for the development of optimal HIV drugs. *Curr. Opin. HIV AIDS* **2019**, *14*, 143-149.
8. M. S. Cohen, Y.Q. Chen, M. McCauley. Prevention of HIV-1 infection with early antiretroviral therapy. *N. Engl. J. Med*. **2011**, *365*, 493-505.
9. C. W. Diffenbach, A. S. Fauci. Thirty years of HIV and AIDS: future challenges and opportunities. *Ann. Intern. Med*. **2011**, *154*, 766-771.
10. P. Braitstein, M. W. G. Brinkhof, F. Dabis, M. Schechter, A. Boulle, P. Miotti, R. Wood, C. Laurent, E. Sprinz, C. Seyler, D. R. Bangsberg, E. Balestre, J. A. C. Sterne, M. May, M Egger. Mortality of HIV-1-infected patients in the first year of antiretroviral therapy: comparison between low-income and high-income countries. *Lancet*, **2006**, *367*, 817-824.
11. K. A. Bosh, A. S. Johnson, A. L. Hernandez, J. Prejean,; J. Taylor, R. Wingard, L. A. Valleroy, H. I. Hall. Vital Signs: Deaths Among Persons with Diagnosed HIV Infection, United States, 2010–2018. *MMWR Morb. Mortal Wkly. Rep*. **2020**, *69*, 1717–1724. DOI: http://dx.doi.org/10.15585/mmwr.mm6946a1
12. Z. Gheibi, Z. Shayan, H. Joulaei, M. Fararouei, S. Beheshti, M. Shokoohi. Determinants of AIDS and non-AIDS related mortality among people living with HIV in Shiraz, southern Iran: a 20-year retrospective follow-up study. *BMC Infect. Dis.* **2019**, *19*, 1094.
13. (a) Z. Lv, Y. Chu, Y. Wang. HIV protease inhibitors: a review of molecular selectivity and toxicity. *HIV AIDS (Auckl)*. **2015**, *7*, 95-107; (b) L. Waters, M. Nelson. Why do patients fail HIV therapy? *Int. J. Clin. Prac.* **2007**, *61*, 983-990.
14. A. Chawla, C. Wang, C. Patton, M. Murray, Y. Punekar, A. de Ruiter, C. Steinhart. A Review of Long-Term Toxicity of Antiretroviral Treatment Regimens and Implications for an Aging Population. *Infect. Dis. Ther.* **2018**, 183-195.
15. C. E. Reust. Common adverse effects of antiretroviral therapy for HIV disease. *Am. Fam. Physician*. **2011**, *83*, 1443-1451.
16. G. Barbaro. Long-term effects of protease-inhibitor-based combination therapy. *The Lancet* **2004**, *363*, 900-901.
17. A. K. Ghosh, B. D. Chapsal. Second-generation approved HIV protease inhibitors for the treatment of HIV/AIDS. In *Aspartic Acid Proteases as Therapeutic Targets*; A. K. Ghosh, Ed.; Wiley-VCH: Weinheim, Germany, **2010**; pp. 169-204.
18. Z. Lu. Second generation HIV protease inhibitors against resistant virus. *Expert Opin. Drug Discov.* **2008**, *3*, 775-786.
19. A. K. Ghosh, D. D. Anderson, I. T. Weber, H. Mitsuya. Enhancing protein backbone binding--a fruitful concept for combating drug-resistant HIV. *Angew. Chem. Int. Ed.* **2012**, *51*, 1778-1802.
20. A. K. Ghosh, B. Chapsal, I. T. Weber, H. Mitsuya. Design of HIV protease inhibitors targeting protein backbone: an effective strategy for combating drug resistance. *Acc. Chem. Res.* **2008**, *41*, 78-86.
21. A. K. Ghosh, J. F. Kincaid, W. Cho, D. E. Walters, K. Krishnan, K. A. Hussain, Y. Koo, H. Cho, C. Rudall, L. Holland, J. Buthod. *Bioorg. Med. Chem. Lett.* **1998**, *8*, 687-690.
22. A. K. Ghosh, Z. L. Dawson, H. Mitsuya. Darunavir, a conceptually new HIV-1 protease inhibitor for the treatment of drug-resistant HIV. *Bioorg. Med. Chem*. **2007**, *15*, 7576-7580.
23. Y. Koh, H. Nakata, K. Maeda, H. Ogata, G. Bilcer, T. Devasamudram, J. F. Kincaid, P. Boross, Y.-F. Wang, Y. Tie, P. Volarath, L. Gaddis, R. W. Harrison, I. T. Weber, A. K. Ghosh, H. Mitsuya. Novel bis-tetrahydrofuranylurethane-containing nonpeptidic protease inhibitor (PI) UIC-94017 (TMC114) with potent activity against multi-PI-resistant human immunodeficiency virus in vitro. *Antimicrob. Agents Chemother.* **2003**, *47*, 3123-3129.
24. S. De Meyer, H. Azijn, D. Surleraux, D. Jochmans, A. Tahri, R. Pauwels, P. Wigerinck, M.-P. de Béthune. TMC114, a novel human immunodeficiency virus type 1 protease inhibitor active against protease inhibitor-resistant viruses, including a broad range of clinical isolates. *Antimicrob. Agent Chemother*. **2005**, *49*, 2314-2321.
25. H. Hayashi, N. Takamune, T. Nirasawa, M. Aoki, Y. Morishita, D. Das, Y. Koh, A. K. Ghosh, S. Misumi, H. Mitsuya. Dimerization of HIV-1 protease occurs through two steps relating to the mechanism of protease dimerization inhibition by darunavir. *Proc. Natl. Acad. Sci. U. S. A.* **2014,** *111*, 12234–12239.
26. Y. Koh, S. Matsumi, D. Das, M. Amano, D. A. Davis, J. Li, S. Leschenko, sA. Baldridge, T. Shioda, R. Yarchoan, A. K. Ghosh, H. Mitsuya. Potent inhibition of HIV-1 replication by novel non-peptidyl small molecule inhibitors of protease dimerization. *J. Biol. Chem*. **2007**, *282*, 28709–28720.
27. A. Y. Kovalevsky, F. Liu, S. Leshchenko, A. K. Ghosh, J. M. Louis, R. W. Harrison, I. T. Weber. Ultra-high resolution crystal structure of HIV-1 protease mutant reveals two binding sites for clinical inhibitor TMC114. *J. Mol. Biol.* **2006**, *363*, 161-173.
28. Y. Tie, P. I. Boross, Y.-F. Wang, L. Gaddis, A. K. Hussain, S. Leshchenko, A. K. Ghosh, J. M. Louis, R. W. Harrison, I. T. Weber. High resolution crystal structures of HIV-1 protease with a potent non-peptide inhibitor (UIC-94017) active against multi-drug-resistant clinical strains. *J. Mol. Biol*., **2004**, *338*, 341-352.
29. A. K. Ghosh, B. D. Chapsal. Design of the anti-HIV protease inhibitor darunavir. In 'From Introduction to Biological and Small Molecule Drug Research and Development' Ed. C. R. Ganellin, S. M. Roberts, R. Jefferis. **2013**, 355-384.
30. M. Aoki, D. Das, H. Hayashi, H. Aoki-Ogata, Y. Takamatsu, A. K. Ghosh, H. Mitsuya. Mechanism of Darunavir (DRV)'s High Genetic Barrier to HIV-1 Resistance: A Key V32I Substitution in Protease Rarely Occurs, but Once It Occurs, It Predisposes HIV-1 To Develop DRV Resistance. *mBio* **2018**, *9*, e02425-17.
31. J. Mallolas. Darunavir Stands Up as Preferred HIV Protease Inhibitor. *AIDS Rev*. **2017**, *19*, 105-112.
32. A. Curran, E. R. Pascuet. [Darunavir as first-line therapy. The TITAN study]. *Enferm. Infecc. Microbiol. Clin*. **2008**, *10*, 14-22.
33. S. De Meyer, E. Lathouwers, I. Dierynck, E. De Paepe, B. Van Baelen, T. Vangeneugden, S. Spinosa-Guzman, E. Lefebvre, G. Picchio, M. P. de Béthune. Characterization of virologic failure patients on darunavir/ritonavir in treatment-experienced patients. *AIDS* **2009**, *23*, 1829–1840.
34. A. K. Ghosh, P. R. Sridhar, N. Kumaragurubaran, Y. Koh, I. T. Weber, H. Mitsuya. Bis-tetrahydrofuran: A privileged ligand for darunavir and a new generation of HIV protease inhibitors that combat drug resistance. *ChemMedChem* **2006**, *1*, 939-950.
35. A. K. Ghosh, B. Chapsal, H. Mitsuya. Darunavir, a New PI with Dual Mechanism: From a Novel Drug Design Concept to New Hope Against Drug-Resistant HIV. In 'Aspartic Acid Proteases as Therapeutic Targets' Ed. A. K. Ghosh, Wiley-VCH Verlag GmbH & Co. KGaA: Weinheim, **2010**, 205-243.
36. M. Deininger, E. Buchdunger, B. J. Druker. The development of imatinib as a therapeutic agent for chronic myeloid leukemia. *Blood*, **2005**, *105*, 2640-2653.
37. M. Dohse, C. Scharenberg, S. Shukla, R. W. Robey, T. Volkmann, J. F. Deeken, C. Brendel, S. V. Ambudkar, A. Neubauer, S. E. Bates. Comparison of ATP-binding cassette transporter interactions with the tyrosine kinase inhibitors imatinib, nilotinib, and dasatinib. *Drug Metab. Dispos.* **2010**, *38*, 1371-1380.
38. D. L. DeRemer, C. Ustun, K. Natarajan. Nilotinib: A Second-Generation Tyrosine Kinase Inhibitor for the Treatment of Chronic Myelogenous Leukemia. *Clin. Ther.* **2008**, *30*, 1956-1975.
39. J. Y. Blay, M. von Mehren. Nilotinib: a novel, selective tyrosine kinase inhibitor. *Semin. Oncol.* **2011**, *38*, S3-S9.

40. T. Schindler, W. Bornmann, P. Pellicena, W. T. Miller, B. Clarkson, J. Kuriyan. Structural mechanism for STI-571 inhibition of abelson tyrosine kinase. *Science*, **2000**, *289*, 1938-1942.
41. J. S. Tokarski, J. A. Newitt, C. Y. J. Chang, J. D. Cheng, M. Wittekind, S. E. Kiefer, K. Kish, F. Y. F. Lee, R. Borzillerri, L. J. Lombardo, D. Xie, Y. Zhang, H. E. Klei. The structure of Dasatinib (BMS-354825) bound to activated ABL kinase domain elucidates its inhibitory activity against imatinib-resistant ABL mutants. *Cancer Res.* **2006**, *66*, 5790-5797.
42. A. K. Ghosh, J. Takayama, L. Kassekart, J.-R. Ella-Menye, S. Yashchuk, J. Agniswamy, Y.-F. Wang, M. Aoki, M. Amano, I.T. Weber, H. Mitsuya. Structure-based design, synthesis, X-ray studies, and biological evaluation of novel HIV-1 protease inhibitors containing isophthalamide-derived P2-ligands. *Bioorg. Med. Chem. Lett.* **2015**, *25*, 4903-4909.
43. A. K. Ghosh, M. Brindisi, P. R. Nyalapatla, J. Takayama, J.-R. Ella-Menye, S. Yashchuk, J. Agniswamy, Y.-F. Wang, M. Aoki, M. Amano, I. T. Weber, H. Mitsuya. Design of Novel HIV-1 Protease Inhibitors Incorporating Isophthalamide-Derived P2-P3 Ligands: Synthesis, Biological Evaluation and X-Ray Structural Studies of Inhibitor-HIV-1 Protease Complex. *Bioorg. Med. Chem.* **2017**, *25*, 5114–5127.
44. M. Kozisek, J. Bray, P. Rezacova, K. Saskova, J. Brynda, J. Pokorna, F. Mammano, L. Rulisek. J. Konvalinka. *J. Mol. Biol.* 2007, *374*, 1005-1016.
45. S. W. Kaldor, V. J. Kalish, J. F. Davies, B. V. Shetty, J. E. Fritz, K. Appelt, J. A. Burgess, K. M. Campanale, N. Y. Chirgadze, D. K. Clawson, B. A. Dressman, S. D. Hatch, D. A. Khalil, M. B. Kosa, P. P. Lubbehusen, M. A. Muesing, A. K. Patick, S. H. Reich, K. S. Su, J. H. Tatlock. Viracept (nelfinavir mesylate, AG1343): a potent, orally bioavailable inhibitor of HIV-1 protease. J. Med. Chem. **1997**, **40**, 3979-3985.
46. Z. Wang. Hantzsche Thiazole Synthesis. Chapter 296 in *Comprehensive Organic Name Reactions and Reagents*. John Wiley & Sons Inc. (2010), 10.1002/9780470638859.conrr296.
47. J. G. Schantl, I. M. Lagoja. Expedient Synthesis of N-Substituted 2-Aminothiazoles. *Synth. Commun.* **1998**, *28* (8), 1451–1462.
48. T. W. Bell, F. Sondheimer. Synthesis and Wittig Reaction of 1-(Triphenylphosphoranylidene)-3-Methoxy-2-Propanone. *J. Org. Chem.* **1981**, *46* (1), 217–219.
49. M. V. Toth, G. R. Marshall. A Simple, Continuous Fluorometric Assay for HIV Protease. Int. *J. Pept. Protein Res.* **1990**, *36*, 544-550.
50. Y. Koh, M. Amano, T. Towata, M. Danish, S. Leshchenko-Yashchuk, D. Das, M. Nakayama, Y. Tojo, A. K. Ghosh, H. Mitsuya. In Vitro Selection of Highly Darunavir-Resistant and Replication-Competent HIV-1 Variants by Using a Mixture of Clinical HIV-1 Isolates Resistant to Multiple Conventional Protease Inhibitors. *J. Virol.* **2010**, *84*, 11961-11969.
51. For details of X-ray studies, please see Supplementary Information.
52. A. K. Ghosh, K. V. Rao, P. R. Nyalapatla, S. Kovela, M. Brindisi, H. L. Osswald, B. S. Reddy, J. Agniswamy, Y.-F. Wang, M. Aoki, S.-i. Hattori, I. T. Weber, H. Mitsuya. Design of Highly Potent, Dual Acting and Central Nervous System Penetrating HIV-1 Protease Inhibitors with Excellent Potency against Multidrug-Resistant HIV-1 Variants. *ChemMedChem* **2018**, 13, 803-815.
53. A. K. Ghosh, S. Kovela, H. L. Osswald, M. Amano, M. Aoki, J. Agniswamy, Y.-F. Wang, I. T. Weber, H. Mitsuya. Structure-Based Design of Highly Potent HIV1 Protease Inhibitors Containing New Tricyclic Ring P2-Ligands: Design Synthesis, Biological, and Xray Structural Studies. *J. Med. Chem.*, **2020**, *63*, 4867-4879.
54. J. Agniswamy, D. W. Kneller, R. Brothers, Y-F. Wang, R. W. Harrison, I. T. Weber. Highly Drug-Resistant HIV-1 Protease Mutant PRS17 Shows Enhanced Binding to Substrate Analogues. *ACS Omega* **2019**, *4*, 8707-8719.
55. Z. Otwinowski, W. Minor. Processing of X-ray Diffraction Data Collected in Oscillation Mode. Methods in Enzymology, 276: Macromolecular Crystallography, Part A; Carter, C.W., Jr., Sweet, R. M., Eds.; Academic Press: New York, 1997; pp 307-326.
56. A. J. McCoy, R. W. Grosse-Kunstleve, P. D. Adams, M. D. Winn, L. C. Storoni, R. J.; Read. Phaser Crystallographic Software. *J. Appl. Crystallogr.* **2007**, *40*, 658–674.
57. M. D. Winn et al. Overview of the CCP4 suite and current developments. *Acta Crystallogr., Sect. D: Biol. Crystallogr.* **2011**, *67*, 235-242.
58. Collaborative Computational Project, Number 4, The CCP4 Suite: Programs for Protein Crystallography. *Acta Crystallogr., Sect. D: Biol. Crystallogr.* **1994**, *50*, 760-763.
59. E. Potterton, P. Briggs, M. Turkenburg, E. Dodson. A Graphical User Interface to the CCP4 Program Suite. *Acta Crystallogr., Sect. D: Biol. Crystallogr.* **2003**, *59*, 1131–1137.
60. C.-H. Shen, Y.-F. Wang, A. Y. Kovalevsky, R. W. Harrison, I. T. Weber. Amprenavir Complexes with HIV-1 Protease and its Drug-Resistant Mutants Altering Hydrophobic Clusters. *FEBS J.* **2010**, *277*, 3699-3714.
61. G. N. Murshudov, A. A. Vagin, E. J. Dodson. Refinement of macromolecular structures by the maximum-likelihood method. *Acta. Crystallogr. D Biol. Crystallogr. Part III* **1997**, *53*, 240-255.
62. A. A. Lebedev, P. Young, M. N. Isupov, O. V. Moroz, A. A. Vagin, Murshudov, G. N. JLigand: a graphical tool for the CCP4 template-restraint library. *Acta Crystallogr D Biol Crystallogr., Part IV* **2012**, *68*, 431-440.
63. P. Emsley, B. Lohkamp, W. G. Scott, K. Cowtan. Features and Development of Coot. *Acta Crystallogr., Sect. D: Biol. Crystallogr.* **2010**, *66*, 486-501.
64. P. Emsley, K. Cowtan. Coot: Model-Building Tools for Molecular Graphics. *Acta Crystallogr., Sect. D: Biol. Crystallogr.* **2004**, *60*, 2126–2132.
65. H. M. Berman, J. Westbrook, Z. Feng, G. Gilliland, T. N. Bhat, H. Weissig, I. N. Shindyalov, P. E. Bourne. The Protein Data Bank. *Nucleic Acids Res.* **2000**, *28*, 235–242.

Graphical Abstract

Exploration of Imatinib and Nilotinib-Derived Templates as the P2-Ligand for HIV-1 Protease Inhibitors: Design, Synthesis, Protein X-ray Structural Studies, and Biological Evaluation

Leave this area blank for abstract info.

Arun K. Ghosh, Jennifer L. Mishevich, Satish Kovela, Ryan Shaktah, Ajay K. Ghosh, Megan Johnson, Yuan-Fang Wang, Andres Wong-Sam, Johnson Agniswamy, Masayuki Amano, Yuki Takamatsu, Shin-ichiro Hattori, Irene T. Weber, Hiroaki Mitsuya.